● REVIEW ●

Terrestrial Near-Surface Wind Speed Variations in China: Research Progress and Prospects

Jinlin ZHA[1,2], Deming ZHAO[1*], Jian WU[2], and Cheng SHEN[3]

1 *CAS Key Laboratory of Regional Climate and Environment for Temperate East Asia, Institute of Atmospheric Physics, Chinese Academy of Sciences (CAS), Beijing* 100029
2 *Key Laboratory of Atmospheric Environment and Processes in the Boundary Layer over the Low-Latitude Plateau Region, Department of Atmospheric Science, Yunnan University, Kunming* 650091
3 *Gaochun District Meteorological Office, Nanjing* 211300

(Received September 2, 2020; in final form January 28, 2021)

ABSTRACT

Changes in terrestrial near-surface wind speed (NSWS) are indicative of the concentrated net effect of climate change and anthropogenic activities. Investigating change mechanisms of NSWS not only furthers the understanding of how the atmosphere changes and improves the climate analysis and projection, but also aids the evaluation and application of wind energy resources. Recent advances in studies of the changes and associated mechanisms of the NSWS over China are reviewed in this paper. Some new results have been achieved in understanding the behaviors of the NSWS changes. The NSWS over China has experienced a decrease in the past 40 years and a recovery in the recent decade, exhibiting large regional and seasonal differences. Understanding of the mechanisms of the NSWS changes has been improved in several aspects; for example, it is found that the reduced NSWS over China is due to the weakening of the pressure-gradient force (PGF) attributed to variations in large-scale ocean–atmosphere circulations (LOACs) as well as the increase of surface roughness due to the land use and cover change (LUCC). The main methods used to analyze the NSWS changes and corresponding mechanisms are also elucidated and discussed. However, studies are still lacking on the mechanisms for multi-timescale (seasonal, interannual, decadal, multi-decadal) variations in the NSWS over China, and it remains unknown about the contributions of different forcing factors to the NSWS changes. Finally, key scientific issues regarding our understanding of the NSWS changes are proposed for future investigation.

Key words: near-surface wind speed (NSWS), land use and cover change (LUCC), large-scale ocean−atmosphere circulations (LOACs), detection and attribution, future projection

Citation: Zha, J. L., D. M. Zhao, J. Wu, et al., 2021: Terrestrial near-surface wind speed variations in China: Research progress and prospects. *J. Meteor. Res.*, **35**(3), 537–556, doi: 10.1007/s13351-021-0143-x.

1. Introduction

Wind speed is an important parameter for studying atmospheric dynamics and climate change. Further, near-surface wind speed (NSWS) and its changes are not only intimately related to the atmospheric circulation, climate and climate change, but also relevant to evaluation and development of wind energy resources (Zhang et al., 2009). Investigations of the causes of NSWS variations are required imperatively for assessing many long- and short-term societal and economic issues linked to NSWS.

NSWS has a considerable effect on visibility (Wu et al., 2013; Zhang et al., 2015; Zhang Y. et al., 2020). A decrease in NSWS hampers the dispersal of pollution and reduces the height of the atmospheric boundary layer, thereby reducing NSWS further in a negative feedback mechanism (McVicar and Roderick, 2010; Sterk et al., 2015). Wind power is a renewable energy resource that is being used increasingly to provide electricity (Pryor and Barthelmie, 2011). Changes in NSWS directly determine the evaluation and development of wind power. A decrease of 1%–5% in NSWS could cause a loss of 1.7%–8.6% in wind energy (He et al., 2010). NSWS changes also influence global and regional evapotranspiration and water circulation (Rayner, 2007; Roderick et al., 2007; McVicar et al., 2008; McInnes et al., 2011;

Supported by the National Key Research and Development Program of China (2018YFA0606004 and 2016YFA0600403), National Natural Science Foundation of China (42005023, 41875178, 41775087, and 41675149), and China Postdoctoral Science Foundation (2019M660761).

*Corresponding author: zhaodm@tea.ac.cn

Niyogi et al., 2011; McVicar et al., 2012a, b; McMahon et al., 2013; Liu et al., 2014). Results show that 65% of the reduction in evaporation is due to reduced NSWS from 1960 to 1991 (Liu et al., 2010, 2011a, b). Accordingly, it is important to study the changes in NSWS because they are related closely to daily human activities.

Given the increased global temperature and intensified human activities affecting the climate, relevant analysis has focused more on temperature and precipitation but less on NSWS in China. The literature to date lacks reviews of progress on studies of NSWS and associated prospects of future research on NSWS across China. To fill the gap, this paper focuses exclusively on changes in NSWS over China. Although the characteristics and causes of changes in NSWS at global scale have been reviewed by Wu et al. (2018a), the present review is special in the following aspects.

(1) It provides detailed information on changes in NSWS over China, such as the variations for different NSWS categories, characteristics of NSWS recovery, and projections of future NSWS changes.

(2) It discusses the credibility of datasets and methods used in former studies, such as quality control and homogenization for observational NSWS, and compares the changes in NSWS using different datasets and analytical methods.

(3) It proposes directions for future studies of NSWS changes in China. For example, the correction and homogenization of observational wind data should be carried out, the NSWS results from high-resolution regional climate models (RCMs) should be evaluated, the contributions of external and natural forces to variations in NSWS must be quantified, and the variations and mechanisms in strong wind and wind gust need to be assessed and so forth.

The paper is organized as follows. Detailed characteristics of changes in NSWS across China are discussed in Section 2. The possible causes of such changes are summarized in Section 3. A discussion is presented in Section 4, and conclusions and future studies are presented in Section 5.

2. Characteristics of changes in NSWS

2.1 *Variations in NSWS outside China: Brief summary*

Studies on wind have focused mainly on NSWS. NSWS has decreased by 5%–15% in the midlatitudes of the Northern Hemisphere from 1979 to 2008 (Vautard et al., 2010). The largest decrease was observed in central Asia (−0.16 m s^{-1} $decade^{-1}$), followed by East Asia (−0.12 m s^{-1} $decade^{-1}$) and Europe (−0.09 m s^{-1} $decade^{-1}$), and the smallest decrease was observed in North America (−0.07 m s^{-1} $decade^{-1}$; Vautard et al., 2010). Roderick et al. (2007) referred to this reduction in NSWS as "stilling." At the regional scale, a slowdown of NSWS was also observed. NSWS in the Great Plains of the United States decreased by nearly 20% during the spring of 1971–2000 (Pryor et al., 2009; Green et al., 2012). The downward trend in NSWS over Australia reached −0.17 m s^{-1} $decade^{-1}$ in 1975–2006 (McVicar et al., 2008; Troccoli et al., 2012). In Europe, NSWS in Switzerland decreased by −0.25 and −0.05 m s^{-1} $decade^{-1}$ during the winter and summer of 1960–2006, respectively; and the rate of decrease in NSWS increased with the increasing altitude (McVicar et al., 2010). A decreasing trend in NSWS was also reported in southern and central France over 1974–2002 (Najac et al., 2011) and in Turkey during 1975–2006 (Dadaser-Celik and Cengiz, 2014). In addition to the overall reduction in NSWS, the probabilities of the occurrence of strong winds also showed decreasing trends. For instance, strong winds in the Netherlands decreased by 10% from 1910 to 2010 (Cusack, 2013). The frequency of extreme winds in Spain and Portugal decreased by 1.5 day yr^{-1} during 1961–2014 (Azorin-Molina et al., 2016). The 90th percentile of NSWS showed a decreasing trend in England from 1980 to 2010 (Earl et al., 2013). The trends of regional NSWS during different study periods are summarized in Fig. 1. Most studies present a reduced NSWS at the regional scale, although the study periods and regions are not consistent with one another (McVicar et al., 2012a). The trends in NSWS are not consistent across different study periods and regions, so the differences of the long-term changes in NSWS over different regions are considerable (Wu et al., 2018a).

2.2 *Spatiotemporal variations in NSWS over China*

2.2.1 *Considerable reduction in NSWS across China*

A stilling phenomenon has been observed in China (Li et al., 2004; Ren et al., 2005; Xu et al., 2006; Jiang et al., 2010a; Zha et al., 2017a). The relative change in magnitude of the annual mean NSWS decreased by more than 20% in most regions of China from 1966 to 2011, and strong reduction was found over Northwest China, Songhuajiang River, Yangtze River, and the river basins of Southeast China, which reached up to 80% (Fig. 2a; Liu et al., 2014). The trends of NSWS are sensitive to the selected time periods (Fu et al., 2011). The magnitudes of decreasing trends in NSWS vary among different studies because different periods, datasets, and methodologies are used. From 1951 to 2000, NSWS decreased by −0.11 m s^{-1} $decade^{-1}$ based on the observed data (Wang et al., 2004). For 1956–2004, the annual

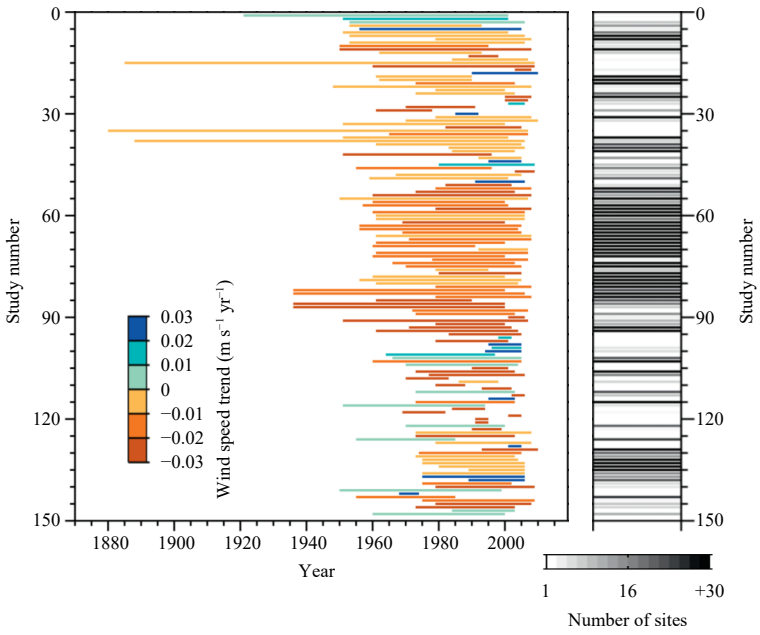

Fig. 1. Change trends of near-surface wind speed (NSWS) over different regions (sites) of the globe based on a review and synthesis of 148 regional studies (from McVicar et al., 2012a, with study number defined in their Table 2).

mean NSWS decreased by −0.12 m s^{-1} decade^{-1} (Jiang et al., 2010a). From 1969 to 2005, the decreasing trend of the annual NSWS was −0.18 m s^{-1} decade^{-1} (Guo et al., 2011). Several studies discovered that the decreasing trend in the annual mean NSWS was −0.07 m s^{-1} decade^{-1} during 1960–2007 (Yin et al., 2010a, b; Liu et al., 2011a, b). The results concerning the trends in NSWS over China for different regions and time periods are summarized in Fig. 2b, with detailed information given in Table 1. Most studies have found a stilling in many regions of China in the past 40 years, although the magnitudes of the weakening NSWS trends vary in different studies.

Some studies have pointed out that the reduction of NSWS is mainly reflected in the reduction of wind strength (Xu et al., 2006; Guo et al., 2011). For instance, gentle breezes (3.4–5.4 m s^{-1}) and moderate breezes (5.5–7.9 m s^{-1}) were reduced by 2.2% and 1.0% decade^{-1} during 1981–2011, respectively (Zha et al., 2016); however, the slowdown in NSWS did not occur in weak winds, and the probabilities of light air (0.3–1.5 m s^{-1}) and light breeze (1.6–3.3 m s^{-1}) showed increasing trends, at the rate of 1.1% and 3.1% decade^{-1}, respectively (Fig. 3). Hence, the variations of different NSWS categories are not the same. A decrease in NSWS does not mean that all wind categories have decreased. The average NSWS mainly reflects the seasonal, interannual, and decadal variations, which cannot reveal the detailed characteristics of variations in NSWS ranges. Hence, studies on different wind categories are helpful in understanding the refined attributes of changes in NSWS.

2.2.2 *Regional and seasonal changes in NSWS*

Regional differences of changes in NSWS are considerable (Shi et al., 2015). Large NSWS values were found in coastal regions and northern China, where the mean NSWS exceeded 2.0 m s^{-1}. Small NSWS values were detected over the Tibetan Plateau, middle reaches of the Yangtze River, and southwestern and southeastern China, where the NSWS was lower than 1.8 m s^{-1} (Jiang et al., 2010a). The spatial pattern of NSWS trends was consistent with that of the mean NSWS, in which strong decreasing trend was accompanied by large NSWS and weak decreasing trend was accompanied by small NSWS. The reduction in NSWS was more significant in northern China than that in southern China (Yin et al., 2010a). The most significant reductions in NSWS were mainly located in northwestern China (McVicar et al., 2010; Lin et al., 2013), followed by northeastern China as well as the middle and lower reaches of the Yangtze River (Wang et al., 2004). To evaluate the impact of climate backgrounds on NSWS, variations of NSWS in several climate zones of China have been studied (Bian et al., 2013; Zheng et al., 2013). The results showed that differences of the changes in NSWS were considerable over different zones: the strongest slowdown was in the extratropical monsoon region, and the weakest slowdown was in the subtropical monsoon region (Zha et al., 2017b). The NSWS over the Tibetan Plateau had a decreasing trend (Yang et al., 2011; Lin et al., 2013); however, the humidity condition and elevation of the

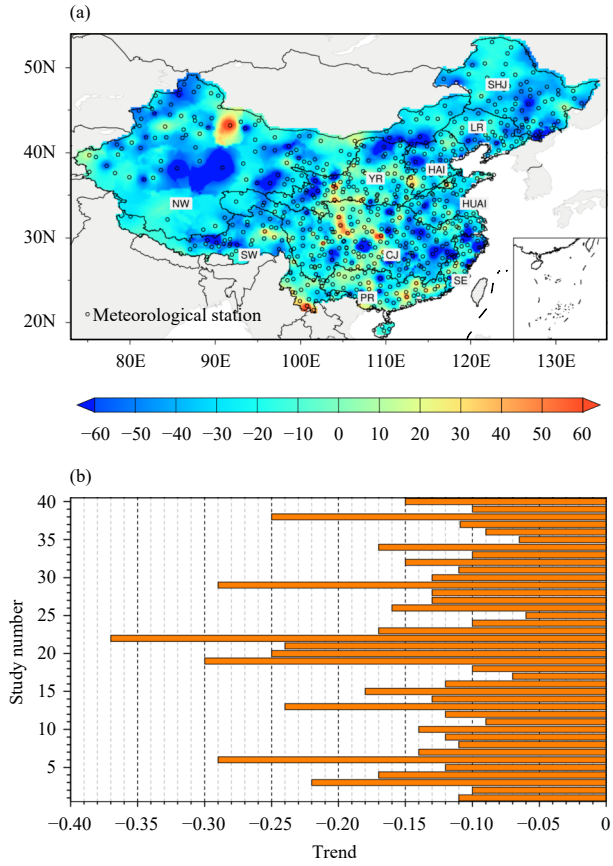

Fig. 2. (a) Distribution of relative change in magnitude (%) of the annual mean NSWS from 1966 to 2011 in China, overlapped with major river basins/regions of China (NW: Northwest China; YR: Yellow River; HAI: Haihe River; LR: Liao River; SHJ: Songhuajiang River; SW: Southwest China; CJ: Yangtze River; HUAI: Huai River; PR: Pearl River; SE: Southeast China). (b) Trends of observational NSWS (m s^{-1} $decade^{-1}$) across different regions in China. The study number is given in Table 1. Panel (a) is taken from Liu et al. (2014).

Tibetan Plateau need to be considered in assessing the NSWS trend. The decrease of NSWS in the arid areas of the Tibetan Plateau was stronger than that in the humid areas (Yang et al., 2011), and was also greater over the high elevation areas around the Tibetan Plateau than those over the low elevation areas (Guo et al., 2017).

Seasonal differences of changes in NSWS are also considerable (Wang et al., 2004; Jiang et al., 2010a). From 1951 to 2000, across the whole of China, the most significant decrease in NSWS was observed in winter (−0.14 m s^{-1} $decade^{-1}$), followed by spring (−0.12 m s^{-1} $decade^{-1}$), autumn (−0.10 m s^{-1} $decade^{-1}$), and summer (−0.08 m s^{-1} $decade^{-1}$). In Hexi Corridor, the maximum NSWS occurred in summer (Li et al., 2004), whereas it occurred in spring over the Tibetan Plateau (Lin et al., 2013). Although the downward trends in NSWS for different seasons were pronounced, the trends began to slow down after 1990 (Fig. 4; Guo et al., 2011). It is obvious that NSWS presents seasonal, interannual, decadal, and multidecadal variations; but most studies mainly analyze the trend in NSWS, with the spatiotemporal characteristics of NSWS at multiple timescales rarely investigated. Investigating the multi-timescale variations of NSWS can help to assess many societal and economic issues related to NSWS at different timescales.

2.2.3 *NSWS recovery over China in the recent decades*

A terrestrial stilling has been revealed in the last several decades, but some studies have also discovered a weak increase in NSWS over the past decade (Zeng et al., 2019; Zhang and Wang, 2020). Zeng et al. (2019) termed this increasing trend in NSWS "reversal." The reversal of terrestrial stilling was also reported in China (Fig. 5;

Table 1. A summary of observed NSWS trends (m s^{-1} $decade^{-1}$) in China and its sub-regions over varied time periods, derived from different source studies/references. Note: Beijing–Tianjin–Hebei—BTH; Yangtze River Delta—YRD; Tibetan Plateau—TP; Haihe River basin—HRB

No.	Region (site)	Period	Trend	Reference	No.	Region (site)	Period	Trend	Reference
1	China (729)	1954–2000	−0.11	Wang et al. (2004)	21	Southwest China (110)	1969–2009	−0.24	Yang et al. (2012)
2	China (323)	1951–2002	−0.10	Ren et al. (2005)	22	Southwest China (110)	1969–2000	−0.37	Yang et al. (2012)
3	China (305)	1969–2000	−0.22	Xu et al. (2006)	23	China (540)	1971–2007	−0.17	Chen et al. (2013)
4	TP (75)	1966–2003	−0.17	Zhang et al. (2007)	24	China (472)	1960–2009	−0.10	Lin et al. (2013)
5	China (604)	1960–1999	−0.12	Li Y. et al. (2008)	25	TP (64)	1960–2009	−0.06	Lin et al. (2013)
6	Western deserts (23)	1973–2003	−0.29	Mahowald et al. (2009)	26	China (741)	1966–2011	−0.16	Liu et al. (2014)
7	HRB (45)	1957–2001	−0.14	Zheng et al. (2009)	27	East China (93)	1980–2011	−0.13	Wu et al. (2016)
8	China (317)	1956–2005	−0.11	Cong et al. (2009)	28	East China (93)	1980–2011	−0.13	Zha et al. (2016)
9	China (535)	1956–2004	−0.12	Jiang et al. (2010b)	29	Xinjiang (10)	1984–2013	−0.29	Liu et al. (2017)
10	Loess Plateau (82)	1960–2006	−0.14	McVicar et al. (2010)	30	East China (93)	1980–2011	−0.13	Wu et al. (2017)
11	China (595)	1961–2008	−0.09	Yin et al. (2010a)	31	China (492)	1979–2010	−0.11	Zha et al. (2017a)
12	China (603)	1971–2008	−0.12	Yin et al. (2010b)	32	China (580)	1970–2011	−0.15	Zha et al. (2017b)
13	TP (71)	1980–2005	−0.24	You et al. (2010)	33	BTH (154)	1978–2014	−0.10	Zhou et al. (2017)
14	China (597)	1961–2007	−0.13	Fu et al. (2011)	34	North China (155)	1971–2015	−0.17	Han et al. (2018)
15	China (726)	1969–2005	−0.18	Guo et al. (2011)	35	YRD (128)	1960–2015	−0.065	Li Y. J. et al. (2018)
16	China (518)	1960–1991	−0.12	Liu et al. (2011a)	36	East China (328)	1981–2011	−0.09	Zha et al. (2019a)
17	China (518)	1992–2007	−0.07	Liu et al. (2011b)	37	China (524)	1958–2015	−0.109	Zhang R. H. et al. (2019)
18	HRB (34)	1950–2007	−0.10	Tang et al. (2011)	38	BTH (223)	1980–2016	−0.25	Wang et al. (2020)
19	TP (78)	1984–2006	−0.30	Yang et al. (2011)	39	China (582)	1980–2017	−0.10	Zhang Y. et al. (2020)
20	Northeast China (87)	1961–2010	−0.25	Jin et al. (2012)	40	China (2333)	1960–2017	−0.15	Zhang and Wang (2020)

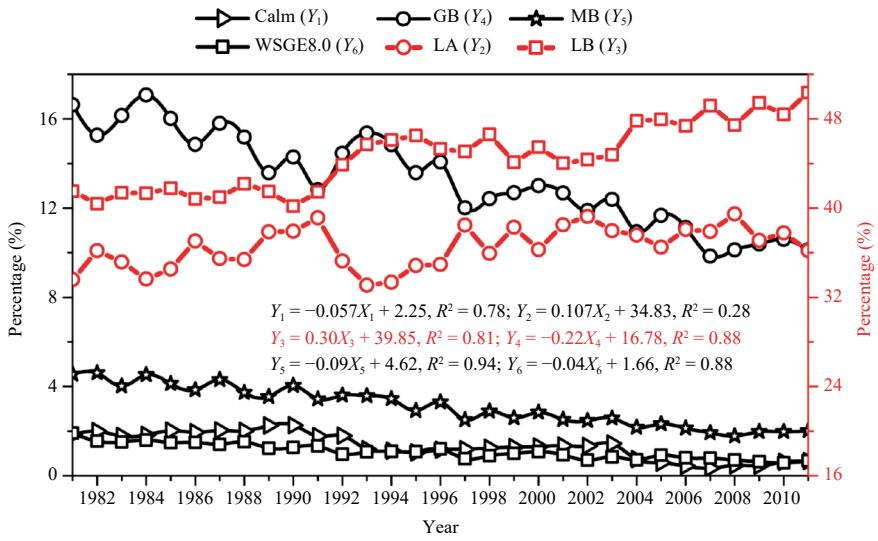

Fig. 3. Temporal changes in probabilities of six wind grades (%) in the observed NSWS across eastern China during 1980–2011. R^2 is the correlation coefficient, which passed the significance *t*-test at the 0.01 level [Calm: 0–0.2 m s^{-1}; LA: light air (0.3–1.5 m s^{-1}); LB: light breeze (1.6–3.3 m s^{-1}); GB: gentle breeze (3.4–5.4 m s^{-1}); MB: moderate breeze (5.5–7.9 m s^{-1}); WSGE8.0: wind speed ≥ 8.0 m s^{-1}]. Adopted from Zha et al. (2016).

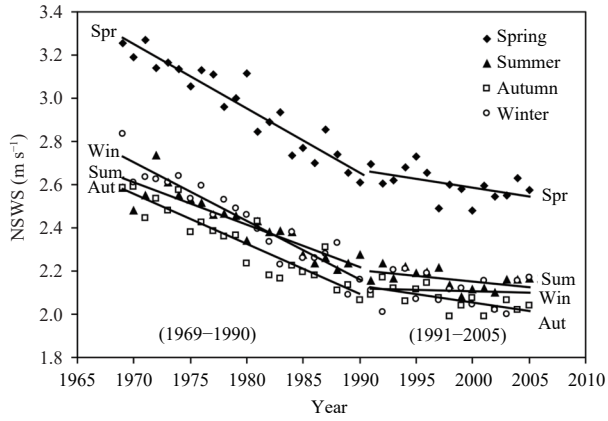

Fig. 4. Temporal variations and trends (solid lines) in seasonal mean NSWS across China from 1969 to 2005 (from Guo et al., 2011).

Zhang and Wang, 2020); however, the magnitudes and turning points of stilling are different due to differences in study regions, periods, datasets, and methods. Yang et al. (2012) analyzed the spatiotemporal characteristics of NSWS over southwestern China and found that NSWS increased after 2000 at rates of 0.60, 0.13, 0.82, and 0.65 m s^{-1} decade^{-1} in winter, spring, summer, and autumn, respectively. An increase in NSWS was also observed over northwestern China from 1993 to 2005, with a trend of 0.04 m s^{-1} decade^{-1} (Li Y. P. et al., 2018). Zha et al. (2019a) revealed a reversal of stilling in winter over eastern China since 2000 (0.0008 m s^{-1} decade^{-1}). Potential causes for NSWS recovery include the increasing temperature difference between high and low latitudes (Yang et al., 2012; Li Y. P. et al., 2018), increasing sea-level pressure at high latitudes (Zha et al., 2019a), and increasing intensity of the Aleutian low over North Pacific (Zhang and Wang, 2020). The stilling and reversal could be a cyclical, decadal pattern of NSWS. However, recent studies mainly analyzed the trends in NSWS in China over the past several decades, while the multidecadal characteristics of NSWS have yet to be revealed. Furthermore, all studies have used the correlation analysis to discuss the causes of NSWS recovery in the recent decades, and the corresponding mechanisms were not revealed in detail. A reversal in terrestrial stilling and the corresponding mechanisms need to be revealed systematically in the future.

2.2.4 *Projection of changes in NSWS across China*

Unlike research on historical NSWS, projection of changes in NSWS has been done rarely in China. It is especially important to select credible models to predict future changes in NSWS. To date, the arithmetic-mean ensemble method is mainly use to project such changes (Jiang et al., 2009, 2010b, 2010c, 2017, 2018; Jiang and Tian, 2013). The errors between observations and different models are different. Based on the arithmetic-mean ensemble method, a model with large errors has the same effect on the ensemble results as a model with small errors. To correct this, relative error between the observation and model is used as weighting coefficient of the model, and weighted ensemble mean is applied. It is thus found that NSWS will increase in the next two decades under the Representative Concentration Pathways 4.5 (RCP4.5) and RCP8.5 scenarios. Furthermore, based on statistical downscaling, the weakening trend in NSWS under RCP8.5 is 3.5 times greater than that under

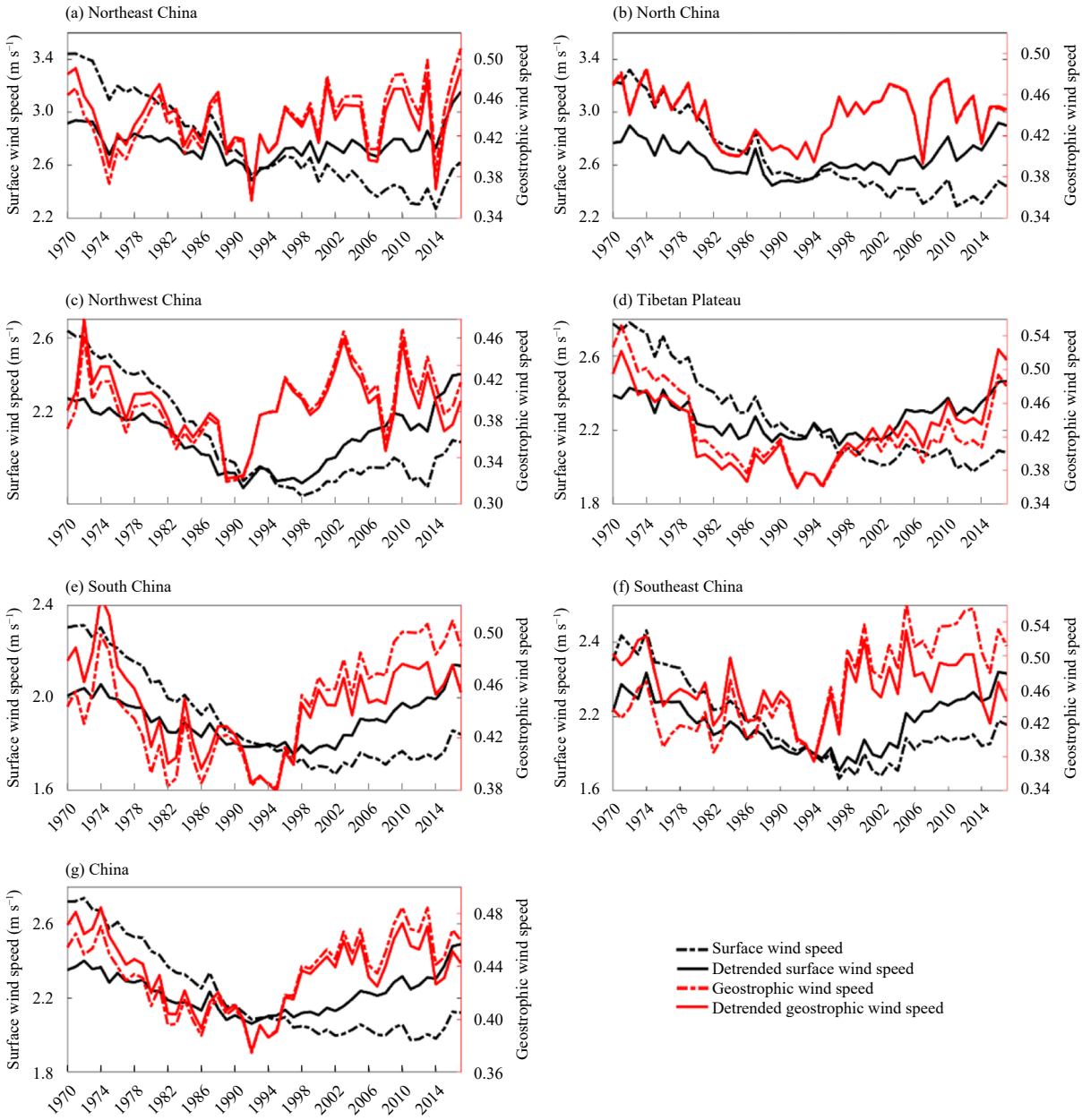

Fig. 5. Time series of the annual mean NSWS and normalized near-surface geostrophic wind across (a–f) six sub-regions and (g) China from 1970 to 2017 (from Zhang and Wang, 2020).

RCP4.5 (Zha et al., 2020). Similar results are also reported by Jiang et al. (2009, 2017, 2018) and Chen et al. (2012). The above studies mainly analyzed the performance of models in simulating long-term trends in NSWS. The ability of the models to simulate seasonal, interannual, decadal, and multidecadal variations in NSWS, as well as the causes of the differences in multi-timescale variations in NSWS between models and observations, has not yet been examined. In addition, the Coupled Model Intercomparison Project phase 3 (CMIP3) and phase 5 (CMIP5) do not perform well in reproducing the past long-term decreasing trends in NSWS (Chen et al., 2012; Jiang et al., 2018; Zha et al., 2020). Why cannot the CMIP models effectively capture the significantly decreasing trends in the observed NSWS? This needs to be investigated systematically, to reduce the uncertainty in NSWS projection.

2.2.5 *Changes of wind energy across China*

It is well recognized that wind power is a virtually carbon-free and pollution-free electricity source, and the global wind resources greatly exceed the electricity demand. Hence, the installed capacity of wind turbines grew at an annual rate of > 20% from 2000 to 2019 and is projected to increase by a further 50% by the end of

2023 (Pryor et al., 2020). As a response to the development, wind power assessment and wind energy industry have received much attention in China (Li et al., 2007). The cumulative installed capacity of wind energy amounted to 180.4 GW by the end of 2015; the newly installed capacity reached 30.5 GW, which accounted for about 48.4% of new windmills globally (Zhang D. H. et al., 2017). Accompanied by the reduction in NSWS, wind energy significantly decreased across most regions of China. The mean wind energy decreased by −3.84 W m^{-2} $decade^{-1}$ due to changes in anthropogenic land use, which was close to the observed climate change (−4.51 W m^{-2} $decade^{-1}$; Li Y. et al., 2008). The significant decreases of wind-generated electricity were mainly found in western Inner Mongolia and northern Gansu, which are the two leading wind energy investment areas, with a decrease of −15% ± 7% and −17% ± 8%, respectively (Sherman et al., 2017). It is worth noting that the projected wind power density in northern China could increase by about 0.7% in the middle of the 21st century if greenhouse gas emissions stay at current levels, but could drop significantly by about −3.32% at the end of the century. Additionally, seasonal differences of changes in future wind energy are considerable. Winter wind energy is projected to increase significantly, and spring and summer wind energy resources are projected to generally decrease (Chen et al., 2020). Further details on wind energy and its demands and changes can be found in Yang et al. (2017) and Pryor et al. (2020).

3. Causes of variations in NSWS across China

3.1 *Variations in the large-scale ocean–atmosphere circulations (LOACs)*

Changes in NSWS are due to changes in the driving force from LOACs, which are under the global warming background. A relationship between a decrease in NSWS and an increase in air temperature has been noted across China (Fig. 6a; Jiang et al., 2010a). The correlation between NSWS and air temperature reached −0.7 ($p < 0.01$), with a 1°C increase in temperature causing a 0.34 m s^{-1} decrease in NSWS (Fig. 6b; Xu et al., 2006). Under global warming, the difference in air temperature between land and ocean, and the difference in sea-level pressure between East Asia and Pacific decrease, which may induce a decrease in NSWS. Nevertheless, the effects of increase in temperature on the reduction in NSWS were only evident via correlation analysis, and the corresponding mechanisms are yet to be explored. Furthermore, the phase variations between NSWS and temperature are different. Therefore, changes in NSWS cannot be accounted for by using air temperature alone.

How LOACs influence NSWS can be revealed by the relationship between climate indices and NSWS. Fu et al. (2011) proposed that NSWS variations across China are related to the interdecadal Pacific oscillation (IPO): positive IPO phases are associated with a significant reduction in NSWS, whereas negative IPO phases are usually not accompanied by a reduction in NSWS. Furthermore, the magnitude of the NSWS trend is much larger during a positive IPO phase than during a negative IPO phase. It should be noted that the spatial pattern of the differences in NSWS trend between positive and negative IPO phases is different—the positive and negative differences in trend are mainly located in western and eastern China, respectively. A reduced NSWS could also be attributed to a decline in East Asian monsoons (Xu et al., 2006). The decline in the East Asian winter monsoon is associated with global-scale warming, while the decline in the East Asian summer monsoon is associated with local cooling over south–central China. Changes in NSWS have displayed multi-timescale characteristics,

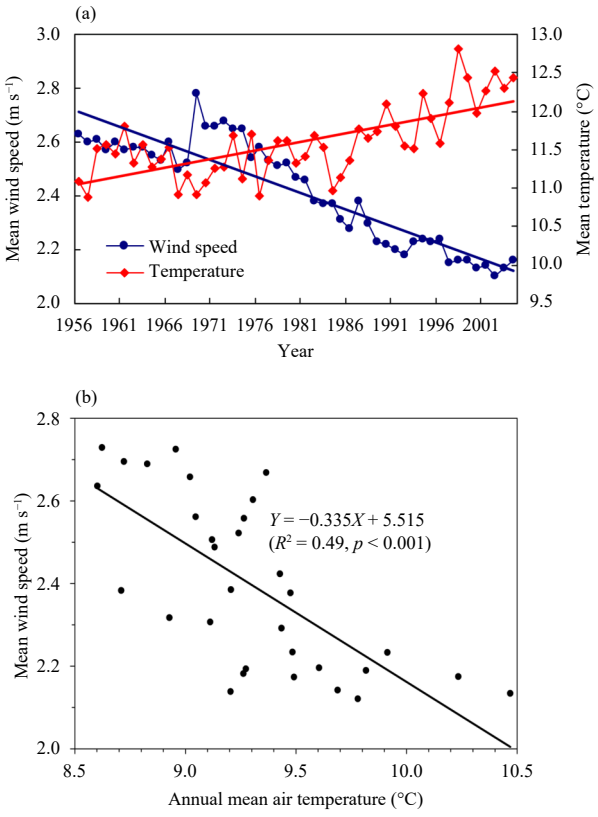

Fig. 6. (a) Temporal changes of annual mean NSWS (m s^{-1}) and temperature (°C) over China from 1956 to 2004. (b) Relationship between the annual mean NSWS and temperature over China during 1969–2000. Panel (a) is from Jiang et al. (2010a) and (b) from Xu et al. (2006).

which could be controlled by different LOACs on different timescales. For instance, from 1979 to 2010, the decadal variability in NSWS over eastern China was controlled mainly by the Pacific decadal oscillation (PDO), with a positive correlation of 0.74; whereas the interannual variability in NSWS was determined by the Northern Hemisphere annular mode (NAM), with a negative correlation of −0.40 (Wu et al., 2018b). Moreover, the interannual variations in spring NSWS in the agro-pastoral transitional zone of northern China were related to the sea surface temperature over North Atlantic and North Pacific (Hu et al., 2019). Since the interaction and modulation among different LOACs are considerable, it is difficult to isolate and quantify the contributions of different LOACs to NSWS changes and reveal the corresponding mechanisms.

LOACs can cause variations in the pressure-gradient force (PGF), which is the driving force of NSWS changes. Some studies have compared NSWS with the PGF. The observed NSWS decrease across the Tibetan Plateau from 1980 to 2005 was caused by a reduced zonal PGF, with a correlation coefficient of 0.88 ($p < 0.01$). Meanwhile, both the geostrophic wind speed (GWS; determined by PGF) at 850 hPa and the NSWS slowed down in spring and summer over China from 1969 to 1990. Therefore, it is proposed that a decreased PGF in the lower troposphere is the leading factor in the decrease of NSWS (You et al., 2010; Guo et al., 2011; Lin et al., 2013). Nevertheless, the changes of PGF at 850 hPa were not consistent with NSWS at near surface (Wu et al., 2016), and the decreasing trends in GWS were much weaker than those in NSWS (Fig. 7; Zhang and Wang, 2020). Accordingly, variations in high-level circulation fields cannot be used to determine changes in NSWS due to NSWS being sensitive to regional climate changes and underlying surface conditions. Moreover, the changes of LOACs are influenced by both natural and anthropogenic forces—How they affect NSWS is yet to be quantified. Previous studies have analyzed how LOACs affect NSWS, but the effects of LOACs on NSWS changes remain to be confirmed and quantified.

3.2 *Land use and cover change (LUCC)*

LUCC in China has been demonstrated significantly (Asselen and Verburg, 2013). From 1990 to 2010, China lost more than 10% of its arable land and saw its total urban area expanded by more than 20% (Liu and Tian, 2010), with approximately 3.18×10^6 hm^2 of arable land used for construction (Liu et al., 2014). In particular, the total area of built-up land increased by 1.76×10^6 hm^2 before 2000 and 3.76×10^6 hm^2 after 2000. Some studies have shown that LUCC influences regional climate change, and it cannot be ignored in climatic change studies (Zhao and Zeng, 2002; Gao et al., 2003; Feddema et al., 2005; Han et al., 2016; Zhao and Wu, 2017a).

To analyze how LUCC (including urbanization) affects NSWS across China, most studies compare the NSWSs of urban stations with those of rural stations using the urban minus rural (UMR) method. The NSWSs of large city stations were larger than those of nonurban stations in China (see Fig. 8a; Xu et al., 2006). Similar results are reported by Jiang et al. (2010a), who compared the NSWSs of 174 large cities with those of 180 small cities from 1956 to 2004 (Fig. 8b). The selection criteria of urban and nonurban stations are different among studies, so different results are obtained for the urbanization influences on NSWS. For instance, Guo et al. (2011) discovered that an averaged NSWS at rural stations was larger than that at urban stations by 0.3 m s^{-1}. Zha et al. (2016) found that the difference in NSWS between small and large cities in China from 1979 to 2010 was 0.47 m s^{-1}. Urbanization may have brought down NSWS, since the frequency of the days with strong winds was reduced (−4.7 day decade^{-1}; Wang et al., 2020), and the vertical decline rate in NSWS grew with the development of urbanization (Xu et al., 2009; Zha et al., 2017a).

How urbanization and other land surface changes influence NSWS can also be examined based on the results of observation minus reanalysis (OMR) because the reanalysis data were less insensitive to changes in the underlying surface (Kalnay and Cai, 2003; Lim et al., 2005). Based on the OMR method, the significant decrease in NSWS over China from 1960 to 1999 can be attributed to anthropogenic LUCC (Li Y. et al., 2008). LUCC could have caused a decrease in NSWS by 0.11 m s^{-1} decade^{-1} from 1979 to 2010, with an estimation error of 10% (Zha et al., 2017a). Furthermore, the decrease in NSWS is closely related to the rate of urbanization, i.e., stronger NSWS decrease usually corresponds to faster urbanization (Li Z. Q. et al., 2018). Because of the coarse resolution of global climate models (GCMs) used by reanalysis, it is difficult for reanalysis to depict accurate regional climate (Kirchmeier et al., 2014; Huang et al., 2015); hence, the OMR method shows considerable uncertainty. Consequently, a downscaling technique is developed to effectively detect regional or local-scale climate signals. Wu et al. (2017) used the statistical downscaling method to downscale the ECMWF reanalysis (extended back to January 1979; ERA-Interim) from January 1989 onward. They estimated the impacts of LUCC on NSWS over eastern China and suggested that every

10% increase in the urbanization rate caused a 0.12 m s^{-1} decrease in NSWS.

In most studies, the effects of LUCC on NSWS reduction across China have been investigated mainly based on correlation analysis. Wu et al. (2016) isolated and quantified the contributions of PGF and LUCC to changes in NSWS and proposed an explanation. From 1980 to 2011, the actual PGF increased with a mean value of 4.1 × 10^{-4} N (Fig. 9a). Influenced by the PGF, wind speed (named as model wind speed) increased, and the changes in model wind speed were consistent with the changes in PGF (Fig. 9c). However, long-term

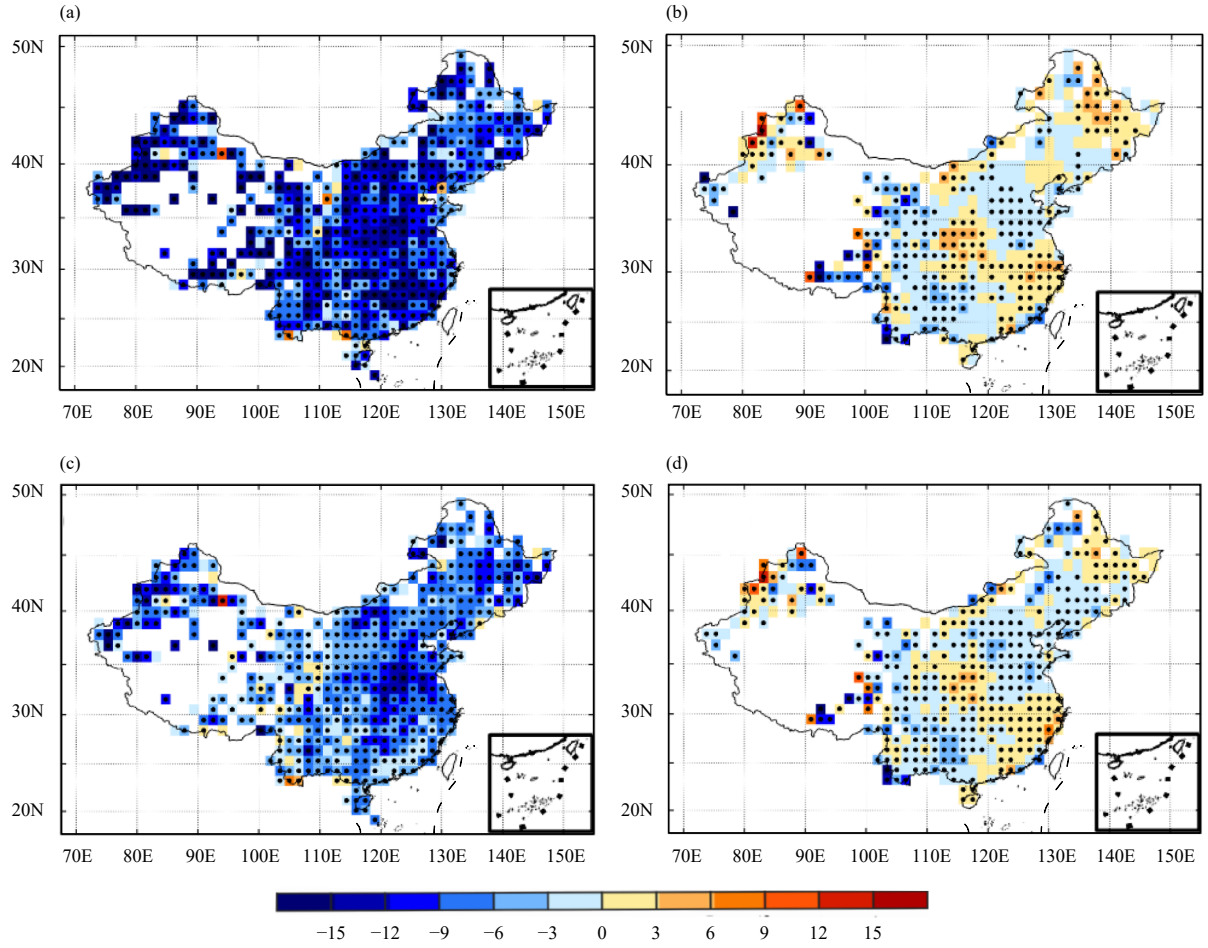

Fig. 7. Normalized linear trends (% $decade^{-1}$) of (a, c) NSWS and (b, d) near-surface geostrophic wind speed (GWS) in different periods across China. (a, b) 1970–2004 and (c, d) 1960–2017. The black dots indicate areas that pass the 95% confidence level in the Mann–Kendall test. Adopted from Zhang and Wang (2020).

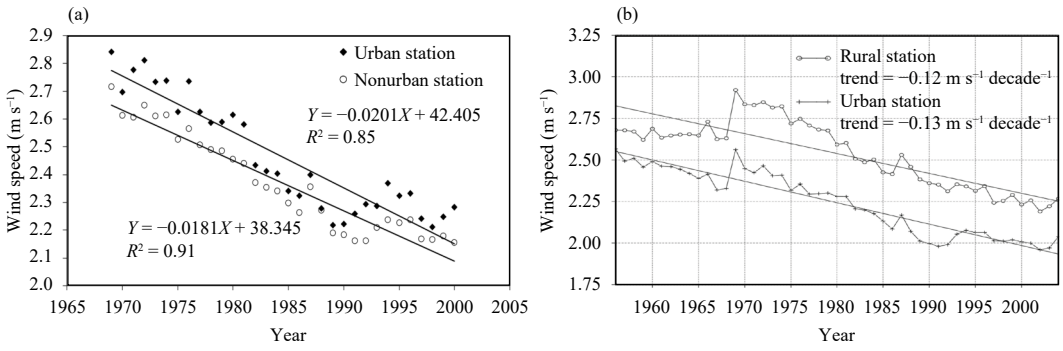

Fig. 8. Temporal changes of NSWS at (a) 30 large cities and 275 nonurban stations in China from 1969 to 2000, and (b) 174 large city stations and 180 small city stations in China from 1956 to 2004. Panel (a) is from Xu et al. (2006) and (b) from Jiang et al. (2010a).

changes in model wind speed were not consistent with those in observations. These results imply that the PGF was not the only factor in the reduced NSWS. On the other hand, it was found that the long-term changes were consistent with the changes in urbanization rate, i.e., expanded urbanization brought about increased drag coefficient, leading to reduced NSWS (Fig. 9b). The estimated result based on friction wind model (FWM) was similar to that based on OMR (Fig. 9d). Consequently, the reduced NSWS across eastern China could be attributed to the increased drag coefficient induced by LUCC (Wu et al., 2016). Based on FWM, the probability of an NSWS greater than 3.8 m s^{-1} is only 1.8% when LUCC effects are included, but the probability is 20.6% when LUCC effects are excluded (Zha et al., 2016). As a significant method in evaluating LUCC effects, the FWM has also been used to analyze the contribution of LUCC to changes in NSWS at the global scale (Zhang Z. T. et al., 2019).

The deceleration effects of LUCC on NSWS across China have also been quantified by numerical simulations (Zhao and Wu, 2017b). Zhang et al. (2010) simulated the impacts of urban land cover expansion on regional climate and discovered a 50% drop in NSWS over the Yangtze River Delta, especially for the high-density urban area, reaching 1.5 m s^{-1}. Similar results were also found for the Pearl River Delta, with the difference in NSWS between urban and nonurban areas reaching −0.27 m s^{-1} (Zhang et al., 2015). Wang et al. (2013) also showed that urbanization caused a decrease of approximately 37% in NSWS over the Pearl River Delta. Based on the Weather Research and Forecasting (WRF) model, the ratio of the urbanized area to the Beijing metropolitan area increased from 1.3% to 11.9%, which was speculated to be the cause of a decrease of 0.4 m s^{-1} in the regional mean NSWS (Hou et al., 2013). With the WRF model, Zha et al. (2019b) showed that NSWS based on land-use data for the 2010s was lower than that for the 1980s by −0.17 m s^{-1}; meanwhile, LUCC induced a decrease of 9.0% in the probability of strong wind. The significant reduction in NSWS over the middle reaches of the Yangtze River Delta was induced by changes in closed shrubland and cropland/natural vegetation mosaic to evergreen broadleaf and deciduous broadleaf forests. The slowdown in NSWS across the Shandong Peninsula, the Beijing–Tianjin–Hebei region, and the Pearl River Delta could be attributed to an increase in urban built-up and a decrease in croplands and cropland/natural vegetation mosaic (Zha et al., 2019b). Anthropogenic activities include not only LUCC but also emission of greenhouse gases (GHGs; Zhang J. Q. et al., 2017), as well as releases of anthropogenic aerosols (AAs; Bichet et al., 2012) and anthropogenic heat (AH; Zhang et al., 2015). Previous studies have evaluated the impacts of anthropo-

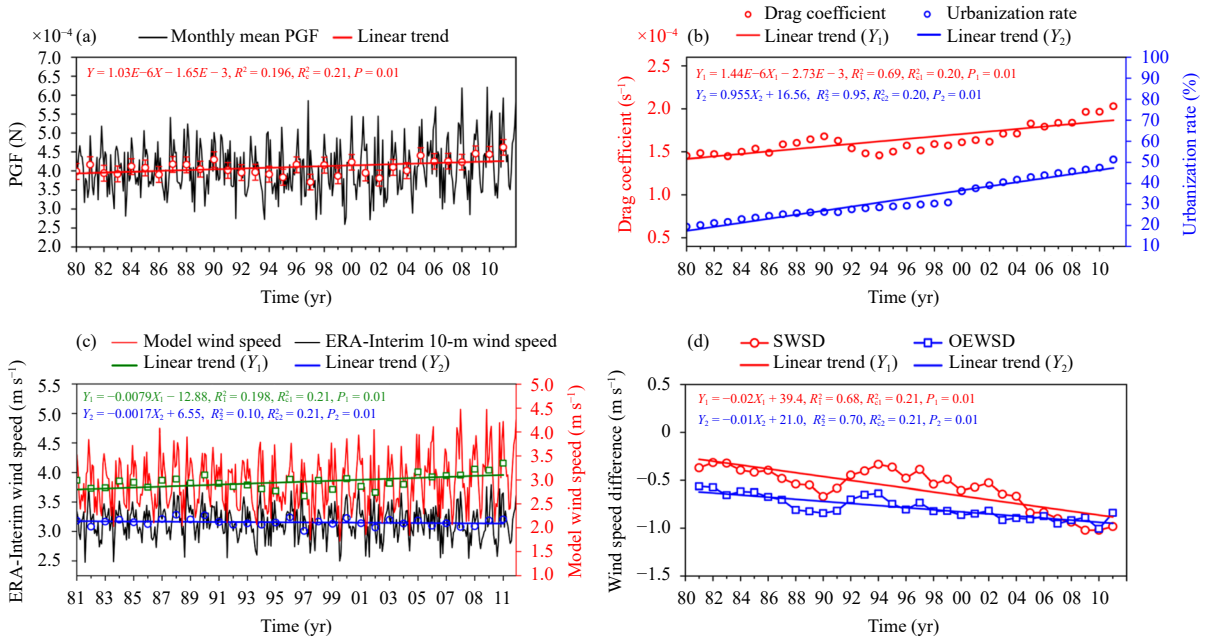

Fig. 9. (a) Temporal changes in the near-surface pressure-gradient force (PGF), (b) annual mean drag coefficient and urbanization rate, (c) model wind speed and ERA-Interim 10-m wind speed, and (d) difference between the observation and model (SWSD) as well as difference between the observation and V10-m-ERA (OEWSD). In (a) and (b), the annual mean values are indicated by rectangles and circles. *R* is the correlation coefficient, *Rc* is the threshold, and *P* is the significance level. In (d), SWSD and OEWSD are obtained by using the FWM and OMR, respectively. Adopted from Wu et al. (2016).

genic LUCC on changes of NSWS, but the contributions of GHGs, AAs, and AH to changes in NSWS are rarely investigated.

3.3 *Other causes*

It is proposed that GHGs can alter the thermodynamics and dynamic processes of the atmosphere and induce NSWS variability (Zhang J. Q. et al., 2017). The AH reduces boundary layer stability and enhances vertical mixing, which leads to an increase in NSWS (Zhang et al., 2015). Some studies hypothesized that aerosols could also influence changes in NSWS. An increase in air stability due to interactions between aerosols and radiation reduces vertical mixing, which in turn reduces the vertical flux of horizontal momentum. Since winds are generally higher aloft than at the surface, weakened vertical mixing reduces the transfer of fast winds aloft to the surface, slowing surface winds compared with those aloft (Li et al., 2016; Zhao et al., 2016). Quantitatively, Jacobson and Kaufman (2006) proposed that an increase in aerosol particles may reduce NSWS by up to 8% locally in China. However, the real physical mechanism of the AAs affecting NSWS has not yet been revealed systematically.

The observed tendencies of NSWS contain, at least partially, the effects of non-climate-related factors (Liu, 2000; Chen et al., 2012). Long-term wind speed series are subject to inhomogeneities resulting from station relocation, anemometer height change, instrumentation change and malfunction, varied sampling interval, and observing environment change (Azorin-Molina et al., 2014). The trends in NSWS are strongly sensitive to such systematic errors (Wan et al., 2010; Li Z. et al., 2011). Winds generally increase with height, i.e., the higher (lower) the anemometer, the larger (smaller) the wind speed. Changes in anemometer location can influence wind speed because NSWS is extremely sensitive to changes in the surface roughness. Unfortunately, the effects of these non-climate-related factors on the slowdown of NSWS across China are rarely estimated.

4. Discussion

4.1 *NSWS data: Quality control and homogenization*

The NSWS datasets were mainly obtained from the China Meteorological Administration (CMA). Related station selection, anemometer installation, and observation procedure were carried out in line with the World Meteorological Organization's standards for the Global Observing System and the CMA's technical regulations on weather observation. Several wind speed datasets have been examined and calibrated by the National Meteorological Information Center of China. On this basis, many studies stated that most observed wind speeds are credible (Xu et al., 2006; Fu et al., 2011; Guo et al., 2011). However, changes in observation instruments were considerable during the period 1967–1970 (Liu, 2000; Fu et al., 2011) although the number of stations with wind speed measurements remained steady after 1970 (Feng et al., 2004). Therefore, to obtain homogeneous wind speed records, the stations must be selected carefully. For instance, the station must be a standard national meteorological station, which never relocate during the study period.

Although the data quality at selected stations is higher than at non-selected stations, an estimation of the significance for the selected stations is necessary because the results are influenced considerably by the inhomogeneity of NSWS data. Inhomogeneities in the long time series of observed winds have been identified by many studies; consequently, quality control and homogeneity testing of the observed NSWS data are necessary (Alexandersson, 1986; Liu, 2000; He et al., 2012). Quality control involves a high–low extreme check, internal consistency check, spatiotemporal outlier check, and missing data check (Feng et al., 2004). Primary homogenization methods include the departure accumulating method (Buishand, 1982), moving *t*-test (Peterson et al., 1998), multiple analysis of series for homogenization (Li Z. et al., 2011), and standard normal homogeneity test (Wu et al., 2018b; Zhang G. F. et al., 2020), and so forth.

4.2 *NSWS in reanalysis data compared with observation*

The NSWS in reanalysis products are compared with observations to estimate the reanalysis' ability in simulating the climatology and long-term trend of NSWS (Wang et al., 2020; Zhang and Wang, 2020). Regarding climatology, the reanalysis datasets had a larger NSWS than observational datasets, except for the Japanese Meteorological Agency 55-yr Reanalysis (JRA55; Fig. 10). Reanalysis datasets, such as the Modern-Era Retrospective analysis for Research and Application (MERRA) and its updated version (MERRA2), the NCEP Climate Forecast System Reanalysis (CFSR), and the ERA-Interim, demonstrated a similar spatial pattern against observations; however, JRA55 exhibited the smallest root-mean square error, followed by CFSR (Chen et al., 2014). For long-term trends, reanalysis products can reproduce NSWS reductions across China, but almost all studies indicate that such reductions in reanalysis datasets are weaker than those in observational datasets (Wu et al., 2016; Zeng et al., 2019; Wang et al., 2020). In the current reanalysis

products, observed NSWS data are assimilated in no other reanalysis products but JRA55, so JRA55 is able to better capture the decreasing trend of NSWS. Therefore, in order to reduce the uncertainties of reanalysis products in simulating the changes in NSWS, observed NSWS data must be considered in the assimilation system in next generation reanalysis products.

Several studies have compared the performance of CMIP models in simulating historical NSWS across China. Zha et al. (2020) discovered that most CMIP5 models had a negative correlation with observation. The standard deviations of NSWS in most CMIP5 models were smaller than those of observation, implying that most CMIP5 models underestimated the interannual and decadal changes in NSWS. Coupled Atmosphere–Ocean General Circulation Models also underestimated the interannual and decadal changes in the observed NSWS (Fig. 11a; Chen et al., 2012). Jiang et al. (2017) evaluated the long-term changes of NSWS in the CMIP5 models with a good performance against observation during 1961–2005 and suggested that CMIP5 models with a good performance underestimated the decreasing trend in NSWS (Fig. 11b). Global reanalysis products are generated at numerical weather prediction centers with advanced data assimilation systems, but most reanalysis products cannot simulate the terrestrial stilling satisfac-

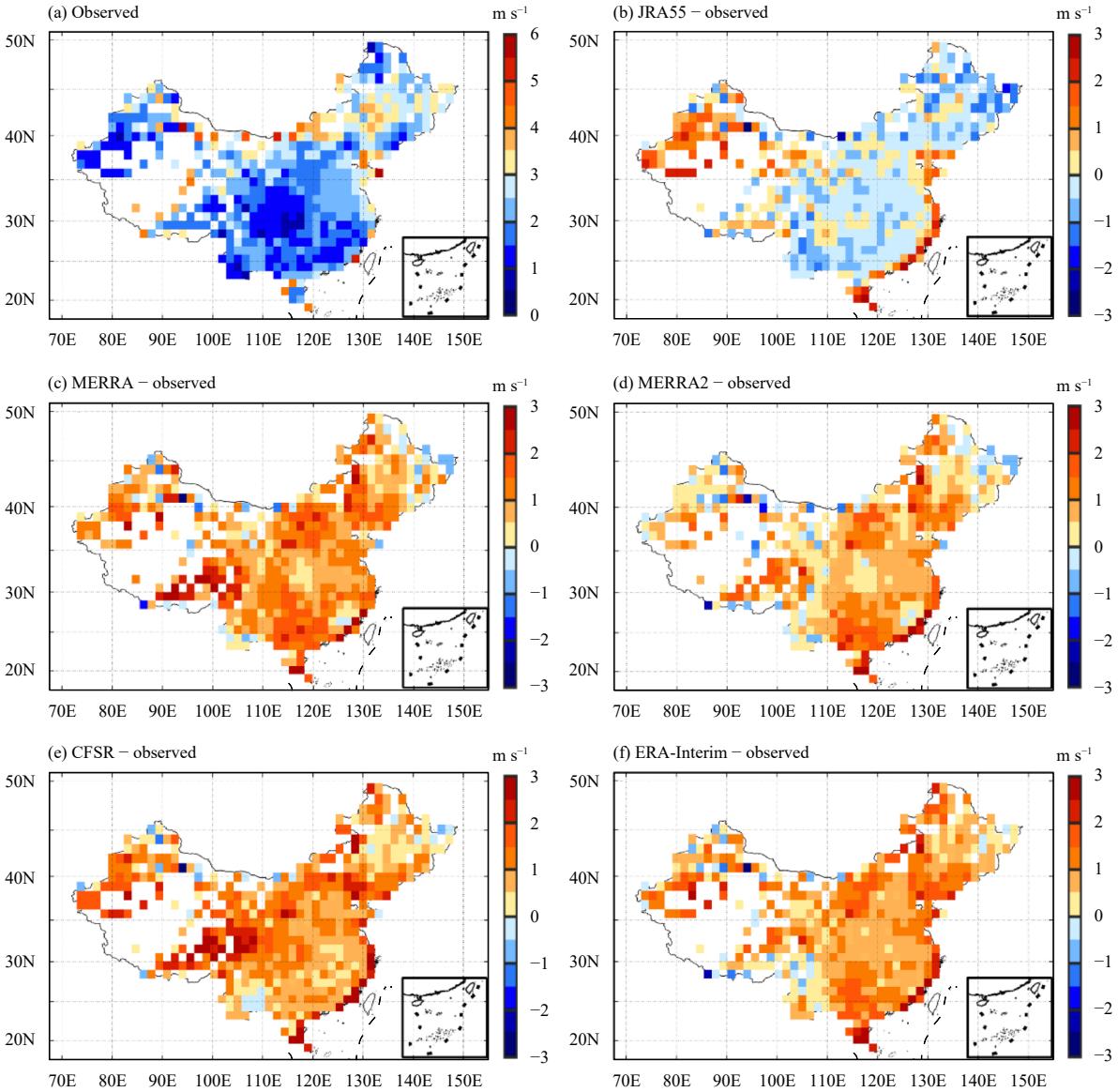

Fig. 10. (a) Observed annual mean NSWS and (b–f) differences of annual mean NSWS between five reanalysis datasets, namely, (b) JRA55, (c) MERRA, (d) MERRA2, (e) CFSR, and (f) ERA-Interim, and the observation, during 1980–2017 in China. Adopted from Zhang and Wang (2020).

torily. Possible reasons for models' failure to reproduce the terrestrial stilling include: 1) considerable decrease in observed NSWS is a manifestation of changes in surface roughness that is not included in the surface boundary conditions used by the climate models; 2) current models only have a relatively weak capacity in representing certain aspects of the atmospheric circulation; 3) the observed trends in NSWS are partly the product of non-climate-related factors, such as inhomogeneities in station settings or instrumentation; and 4) inappropriate model topography and inaccuracies in atmospheric boundary layer processes are implemented into the data assimilation systems of reanalysis products (Chen et al., 2012; Zeng et al., 2019).

Actually, some studies have discovered that in regions where Atmospheric Model Intercomparison Project simulations [atmospheric simulations forced with only the observed sea surface temperature (SST)] capture terrestrial stilling, global reanalysis products are capable of reproducing stilling. In contrast, for regions in which such simulations do not capture stilling, global reanalysis products fail to reproduce stilling. These results imply that a reanalysis product can effectively simulate terrestrial stilling where it can properly simulate the forcing of SST on the atmosphere. In general, NSWS is extremely sensitive to changes in the surface roughness; greater efforts are required to improve surface process parameterization schemes and their connections to ocean–atmosphere circulations in climate models and operational weather data assimilation systems (Zeng et al., 2019).

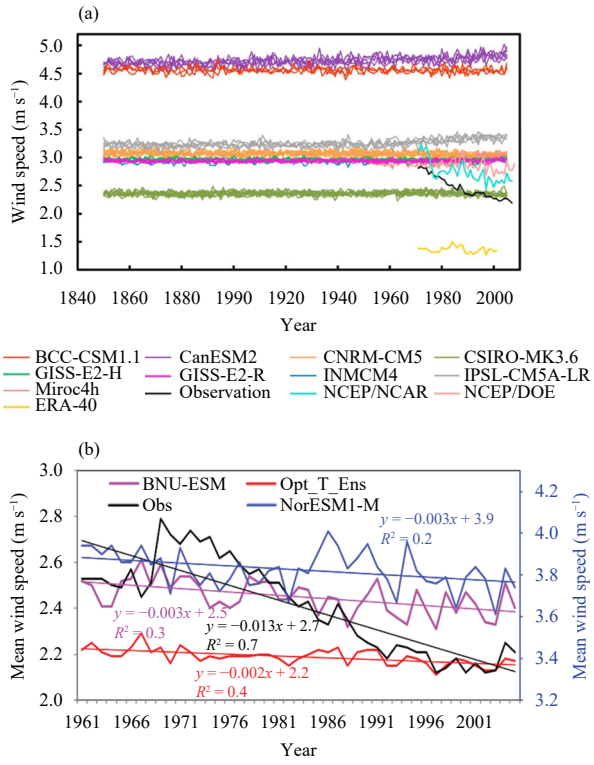

Fig. 11. (a) Annual mean NSWS in China from individual simulations with nine atmosphere–ocean general circulation models (1850–2005) and the time series of mean wind speed from NCEP-NCAR, NCEP-DOE, and ERA-40, as well as the average of the observations. (b) Time series of the annual mean NSWS in observation (Obs: black line), Beijing Normal University Earth System Model (BNU-ESM; purple line), Norwegian Climate Center's Earth System Model (NorESM1-M; blue line), and the ensemble of the models (Opt_T_Ens; red line), in which all time series show decreasing trends in annual mean NSWS except with varying decreasing rates. Panel (a) is from Chen et al. (2012) and (b) from Jiang et al. (2017).

4.3 *Main Methods used for NSWS studies and their limitations*

The main statistical and dynamical methods used to investigate the effects of LOACs on changes in NSWS include the correlation analysis, forward stepwise regression algorithm (FSRA), and geostrophic wind theory.

Correlation analysis is the most widely used method, which can qualitatively describe the relationship between LOACs and NSWS. However, correlation can only analyze the relationship between one ocean–atmosphere oscillation index and NSWS. Changes in NSWS are associated with a combination of variations in various LOACs. The levels of interaction and inter-modulation among different LOACs are considerable. Hence, the mechanisms for the LOACs affecting NSWS are difficult to ascertain by using the correlation analysis.

FSRA can be used to identify the effects of LOACs on NSWS. It is able to recognize primary climate indices, and has the largest potential for analyzing the changes in NSWS (Zeng et al., 2019). FSRA is a systematic method for adding predictors from a linear regression model based on statistical significance. The earlier the climate indices enter the model, the larger the contribution of the climate indices. FSRA can also estimate the relative importance of LOACs to changes in NSWS. Based on FSRA, a reconstructed wind speed can be obtained, including only the effects of LOACs. Comparisons between the reconstructed wind speed and the observed wind speed permit the evaluation of LOAC contributions to changes in NSWS; however, the results depend on selected predictors. Based on different predictors, the estimated results might be different. Furthermore, the physical mechanisms of LOACs affecting NSWS cannot be revealed by FSRA. The use of FSRA has an important presupposition, namely, the predictors are independent and the predictand and predictors satisfy linear relations. In real world, however, such linear relations are

not guaranteed. Whether a nonlinear relation between NSWS and LOACs can better express the effects of LOACs on the NSWS is an interesting issue and needs to be further demonstrated in the future.

Geostrophic wind theory is a mature theory in atmospheric sciences (Wu et al., 2018b; Zhang and Wang, 2020), which can be used to calculate the geostrophic wind ($\boldsymbol{V}_g$). $\boldsymbol{V}_g$ can be used to describe the quantitative effects of PGF on NSWS because it is a direct function of the PGF ($f\boldsymbol{k}\times\boldsymbol{V}_g = \nabla\Phi$, where $\boldsymbol{k}$ is the unit vector in the vertical direction, f is the Coriolis parameter, and $\nabla\Phi$ is the PGF)—$\boldsymbol{V}_g$ has a similar magnitude to that of actual wind (Guo et al., 2011). It should be noted that the observed NSWS cannot be in a quasi-geostrophic equilibrium state, and geostrophic wind theory is mainly used at a high level over the midlatitudes (Guo et al., 2011). The PGF near the surface is not consistent with that at a high level, so the contribution of PGF to changes in NSWS could show a large uncertainty near the surface and low-latitudes based on geostrophic wind theory. Relevant geostrophic wind analysis may only provide limited implications to changes of NSWS.

Main methods used to investigate the effects of LUCC on changes in NSWS across China include the UMR, OMR, FWM, and numerical simulations.

The UMR method has been widely used (e.g., Jiang et al., 2010a; Zha et al., 2016, 2017; Wang et al., 2020) and can be employed when examining the difference in NSWS between urban and rural stations at any scale. Note that economic development is unbalanced in China, with large cities mainly located in eastern China and small cities mainly located in western China. Long-term observations involve very few, strictly rural stations in China. Inhomogeneities in the spatial patterns of large and small cities, and inconsistencies in the selection criteria for urban and rural stations, in different studies, induce large discrepancies in the estimation results. The UMR method cannot determine the effects of LUCC on changes in NSWS at rural stations due to no existence of the reference standard.

The OMR method can be used to quantify the effects of LUCC on long-term changes in NSWS; the effects of LUCC on changes in NSWS in small cities or rural stations can be estimated. However, it is difficult to provide accurate regional and local climate signals to meet the needs of evaluation due to the coarse resolution of GCMs (Fan et al., 2011, 2013; Huang et al., 2015). Therefore, the estimated results could be questionable when the OMR method is used at regional or local scales. The significance of results based on the OMR method could be improved by increasing the resolution in reanalysis data and by using statistical or dynamical downscaling. The statistical and dynamical downscaling methods are valid and effective in diminishing the bias in climate prediction versus observation that is induced by the local characteristics missing in the reanalysis products; thus, downscaling can be used to optimize the reanalysis data to reduce the bias to a minimum. Then, the OMR method can be used to compare the difference between observation and downscaled reanalysis data, with reduced uncertainty (Wu et al., 2017).

FWM is a simple dynamical method, which can be used to isolate the effects of PGF and drag force (Wu et al., 2016; Zhang Z. T. et al., 2019). However, it ignores the effects of turbulent flux and horizontal advection, and it is difficult to use FWM in regions with complex terrain. Furthermore, temporal changes of zonal and meridional winds are not considered in FWM. These factors combine to affect changes in NSWS. Drag force is considered as a simple linear combination of NSWS and drag coefficient; hence, the influence of the drag force on the results remains uncertain (Wu et al., 2018c). In the future, several important parameterization schemes should be introduced to FWM to improve estimation results and isolate the effects of the surface drag and turbulent flux.

Numerical simulations can quantitatively evaluate the contributions of LUCC to changes in NSWS, and can be used to reveal the effects of different land cover types on changes in NSWS (Hou et al., 2013; Zhang et al., 2015; Zhao and Wu, 2017a, b; Zha et al., 2019b). Different numerical experiments elucidate the mechanisms of LUCC affecting changes in NSWS. Due to limitations in computing resources, the previous simulations could be run only on coarse resolutions (Hou et al., 2013; Zhang et al., 2015; Zha et al., 2019b). Therefore, the impacts of various regional and local land type changes on NSWS are ignored. The effects of LUCC mainly present themselves at the decadal scale; thus, numerical experiments must be integrated over a period of a decade or more. Consequently, economic and time costs are significant when many numerical tests are carried out.

5. Conclusions and remarks for future studies

In the last several years, significant advances have been made in studies of the changes in NSWS over China. Almost all the studies show that NSWS in China has been reduced significantly over the past 40 years, with marked regional and seasonal characteristics. However, the results are inconsistent among different studies because of differences in study methods, datasets used,

and time periods selected. Furthermore, a reversal of terrestrial stilling has been found in recent decades across China. NSWS is projected to decrease at the decadal timescale in the future and the downward trend could be strengthened with the increasing GHGs emissions, but the potential mechanisms remain unknown. The causes for the reduction in NSWS are given inconsistently. Some researchers proposed that the slowdown of NSWS across China is due to variations in LOACs under global warming (e.g., East Asian monsoons, PDO, and NAM), whereas others suggested that the slowdown is due to the increasing surface roughness induced by LUCC. Although progress has been made on studies of NSWS in a changing climate in the last few decades, further investigations on understanding the variation in NSWS and its underlying mechanisms are needed—especially investigations that address the following issues.

Wind observations are extremely sensitive to changes in anemometer height and in the location and exposure of the observing site, especially over complex terrains (Wan et al., 2010). Changes in these factors can cause large discontinuities in the wind data series; however, they are often inevitable, especially during a long period of record in China. Therefore, it is not easy to judge which one is correct, the observation or the model, as observational data may also contain large bias resulting from insufficient station representativeness. Consequently, correction and homogenization of wind data are imperative, in particular for assessment of the observed wind speed trends, data assimilation, and model performance. Some homogenization methods, such as the standard normal homogeneity test, the penalized maximal *t* test, the penalized maximal *F* test, the Buishand test, the Pettitt test, the multiple analysis of series for homogenization, and the two-phase regression, can be employed to correct the wind data series. Based on the homogenized NSWS series, the multi-timescale changes (seasonal, interannual, decadal, and multidecadal) in NSWS can be explored, and the key areas of LOACs that significantly affect multi-timescale changes in NSWS across China may be revealed; meanwhile, the contributions of LOACs to these changes can be quantitatively estimated.

The NSWS results from high-resolution RCMs are also important, which may be used in future for the application of NSWS (e.g., evaluation and development of wind energy). High-resolution RCMs are increasingly capable of simulating offshore winds and accurately depicting the influence of complex orography. NSWS is affected by both thermodynamic and dynamic factors. Increasing the horizontal resolution of models can better present the topography and land–sea contrast, which may improve the model performance in simulating the NSWS (Yu et al., 2014; Pryor et al., 2020). Actually, surface winds are much better simulated by a regional model at 6-km grid spacing compared to the reanalysis product at approximately 25-km grid spacing (Pryor et al., 2020). Furthermore, the NSWS simulation also needs to consider the assimilation of observed wind data and the improvement in physical processes, because variations in NSWS could be influenced by cumulus convection, planetary boundary layer, land surface, radiative transfer processes, and many others. The assimilation of observed wind data can correct the systematic errors of models and the improvement in physical processes can well capture some refined physical characteristics. Especially, for the simulation of diurnal cycle of NSWS (Yu et al., 2009, 2010), the improvement in physical parameterization is crucial (Li J. et al., 2008, 2011; Yu et al., 2014). Furthermore, the increasingly large ensembles of high-resolution climate simulations could also better sample uncertainties related to internal variability and model structural uncertainty (Pryor et al., 2020). Land surface is the primary source of drag. LUCC can change the surface roughness, drag coefficient, albedo, and heat exchange, thereby changing the drag from the perspective of dynamics and thermal force. High-resolution RCM can better describe complex topography, so when it is coupled with a GCM and driven by high-precision land-cover data, it could effectively capture the relative contributions of the surface friction and turbulent mixing associated with LUCC to multi-timescale changes in NSWS.

Detection and attribution (D&A) of NSWS changes are required. Based on the results of D&A, an evaluation can be conducted of the contributions of natural forcing, anthropogenic forcing, and internal variability to changes in NSWS. To achieve this goal, several CMIP6 projects will prove useful—for instance, the D&A Model Intercomparison Project (DAMIP) and Land-Use Model Intercomparison Project (LUMIP). Comparative analysis of DAMIP and LUMIP can detect the effects of different external forcings and natural forcings on changes in NSWS (Table 2). Based on experiments using His-nat and historical results, natural forcing and anthropogenic forcing can be divided. Based on experiments in His-nat, His-GHG, His-aer, and historical results, contributions from natural forcing, GHGs, and aerosols to variation in NSWS can be divided.

Projections and corresponding mechanism studies of future changes in NSWS over China are lacking. Projections of NSWS in China would aid the evaluation and exploitation of wind energy, and exploiting and utilizing wind energy will help China to fulfill the Paris Climate

Table 2. A summary of the experiments in Detection and Attribution Model Intercomparison Project (DAMIP) of CMIP6. Refer to Qian and Zhang (2019) for details

Experiment	Experiment description	Simulation period	Minimum ensemble member
CMIP6 historical simulation and SSP2-4.5	Historical climate simulation in CMIP6 (1850–2014) and the SSP2-4.5 scenario simulation (2015–2020)	1850–2020	3
His-nat	Historical simulations involving only natural forcing	1850–2020	3
His-GHG	Historical simulations involving only sufficiently mixed greenhouse gas forcing	1850–2020	3
His-aer	Historical climate simulations involving only anthropogenic aerosol forcing	1850–2020	3
His-sol	Historical climate simulations involving only solar radiation forcing	1850–2020	3
His-volc	Historical climate simulation involving only volcanic forcing	1850–2020	3
His-CO_2	Historical climate simulation involving only CO_2	1850–2020	3
SSP245-aer	Future projections based on the His-aer test accompanied by the aerosol concentration or emission in tropospheric under the SSP2-4.5	2021–2100	1
SSP245-nat	Future projections based on the His-nat test accompanied by solar forcing and volcanic forcing under the SSP2-4.5	2021–2100	1

Agreement and its commitment to reduce emissions. In the mean time, the multi-timescale variations in NSWS need to be projected as well for different emission scenarios, with statistical and dynamical downscaling methods, across China and some representative regions (e.g., the Tibetan Plateau, Yangtze River Delta, Pearl River Delta, Beijing–Tianjin–Hebei region, and arid and semi-arid regions of Northwest China). GCMs with horizontal resolutions of 25–50 km are being included in CMIP6 under high resolution model intercomparison project (HighResMIP) and those with 5-km resolution are being actively developed and tested. These models can accommodate mesoscale and even convection-permitting resolutions in the refined domain while using coarser grid spacing in the outer domain. Hence, projections of NSWS across China and its sub-regions could be carried out based on the HighResMIP.

CO_2 emissions increase air temperature. The related warming is temporally non-synchronized and spatially non-uniform, resulting in spatial differences in temperature changes in the horizontal direction. Accompanied by changes in CO_2 emissions, the spatial difference in temperature could be in different degrees. Changes in NSWS are not consistent with the inhomogeneous warming under different social development scenarios. Investigating the mechanism of future changes in NSWS will need to estimate the performance of the models in simulating the variation in LOACs, as well as to analyze the effects of changes in CO_2 emissions on the primary LOACs, affecting the changes in wind speed over China.

Studies of wind speed changes must consider the variation in the daily maximum wind speed (DMWS) and wind gust because the DMWS and wind gust influence soil erosion, pollutant diffusion, and damage to buildings, infrastructure, and crops, with large concomitant economic losses (Lin et al., 2015; Zhang J. Q. et al., 2017; Zhang G. F. et al., 2019). It is necessary to evaluate multi-timescale variation in DMWS and wind gust, then reveal the mechanisms of DMWS and wind gust changes. The occurrence and evolution of DMWS and wind gust are generated within the mean flows; therefore, to explore DMWS variation, one must compare DMWS with the mean wind field. Additionally, some human activities, such as LUCC and releases of AAs, GHGs, and AH, may influence DMWS and wind gust, especially in mega-city clusters. Future work needs to isolate and quantify the effects of such anthropogenic factors on changes in DMWS and wind gust.

Acknowledgments. This work is also supported by the Special Program for Research Assistants of Chinese Academy of Sciences, Program for Key Laboratories in Universities of Yunnan Province, and Jiangsu Province Collaborative Innovation Center for Climate Change.

REFERENCES

Alexandersson, H., 1986: A homogeneity test applied to precipitation data. *Int. J. Climatol.*, **6**, 661–675, doi: 10.1002/joc.3370060607.

Asselen, S. V., and P. H. Verburg, 2013: Land cover change or land-use intensification: simulating land system change with a global-scale land change model. *Glob. Change Biol.*, **19**, 3648–3667, doi: 10.1111/gcb.12331.

Azorin-Molina, C., S. M. Vicente-Serrano, T. R. McVicar, et al., 2014: Homogenization and assessment of observed near-surface wind speed trends over Spain and Portugal, 1961–2011. *J. Climate*, **27**, 3692–3712, doi: 10.1175/JCLI-D-13-00652.1.

Azorin-Molina, C., J. A. Guijarro, T. R. McVicar, et al., 2016: Trends of daily peak wind gusts in Spain and Portugal, 1961–2014. *J. Geophys. Res. Atmos.*, **121**, 1059–1078, doi: 10.1002/2015JD024485.

Bian, J. J., Z. X. Hao, J. Y. Zheng, et al., 2013: The shift on boundary of climate regionalization in China from 1951 to 2010. *Geogr. Res.*, **32**, 1179–1187. (in Chinese)

Bichet, A., M. Wild, D. Folini, et al., 2012: Causes for decadal variations of wind speed over land: Sensitivity studies with a global climate model. *Geophys. Res. Lett.*, **39**, L11701, doi: 10.1029/2012GL051685.

Buishand, T. A., 1982: Some methods for testing the homogeneity of rainfall records. *J. Hydrol.*, **58**, 11–27, doi: 10.1016/0022-1694(82)90066-X.

Chen, G. X., T. Iwasaki, H. L. Qin, et al., 2014: Evaluation of the warm-season diurnal variability over East Asia in recent reanalyses JRA-55, ERA-Interim, NCEP CFSR, and NASA MERRA. *J. Climate*, **27**, 5517–5537, doi: 10.1175/JCLI-D-14-00005.1.

Chen, L., S. C. Pryor, and D. L. Li, 2012: Assessing the performance of Intergovernmental Panel on Climate Change AR5 climate models in simulating and projecting wind speeds over China. *J. Geophys. Res. Atmos.*, **117**, D24102, doi: 10.1029/2012JD017533.

Chen, L., D. Li, and S. C. Pryor, 2013: Wind speed trends over China: quantifying the magnitude and assessing causality. *Int. J. Climatol.*, **33**, 2579–2590, doi: 10.1002/joc.3613.

Chen, Z., W. Li, J. H. Guo, et al., 2020: Projection of wind energy potential over northern China using a regional climate model. *Sustainability*, **12**, 3979, doi: 10.3390/su12103979.

Cong, Z. T., D. W. Yang, and G. H. Ni, 2009: Does evaporation paradox exist in China? *Hydrol. Earth Syst. Sci.*, **13**, 357–366, doi: 10.5194/hess-13-357-2009.

Cusack, S., 2013: A 101 year record of windstorms in the Netherlands. *Climatic Change*, **116**, 693–704, doi: 10.1007/s10584-012-0527-0.

Dadaser-Celik, F., and E. Cengiz, 2014: Wind speed trends over Turkey from 1975 to 2006. *Int. J. Climatol.*, **34**, 1913–1927, doi: 10.1002/joc.3810.

Earl, N., S. Dorling, R. Hewston, et al., 2013: 1980–2010 variability in U.K. surface wind climate. *J. Climate*, **26**, 1172–1191, doi: 10.1175/JCLI-D-12-00026.1.

Fan, L. J., C. B. Fu, and D. L. Chen, 2011: Long-term trend of temperature derived by statistical downscaling based on EOF analysis. *Acta Meteor. Sinica*, **25**, 327–339, doi: 10.1007/s13351-011-0308-0.

Fan, L. J., D. L. Chen, C. B. Fu, et al., 2013: Statistical downscaling of summer temperature extremes in northern China. *Adv. Atmos. Sci.*, **30**, 1085–1095, doi: 10.1007/s00376-012-2057-0.

Feddema, J. J., K. W. Oleson, G. B. Bonan, et al., 2005: The importance of land-cover change in simulating future climates. *Science*, **310**, 1674–1678, doi: 10.1126/science.1118160.

Feng, S., Q. Hu, and W. H. Qian, 2004: Quality control of daily meteorological data in China, 1951–2000: a new dataset. *Int. J. Climatol.*, **24**, 853–887, doi: 10.1002/joc.1047.

Fu, G. B., J. J. Yu, Y. C. Zhang, et al., 2011: Temporal variation of wind speed in China for 1961–2007. *Theor. Appl. Climatol.*, **104**, 313–324, doi: 10.1007/s00704-010-0348-x.

Gao, X. J., Y. Luo, W. T. Lin, et al., 2003: Simulation of effects of land use change on climate in China by a regional climate model. *Adv. Atmos. Sci.*, **20**, 583–592, doi: 10.1007/BF02915501.

Greene, J. S., M. Chatelain, M. Morrissey, et al., 2012: Estimated changes in wind speed and wind power density over the western High Plains, 1971–2000. *Theor. Appl. Climatol.*, **109**, 507–518, doi: 10.1007/s00704-012-0596-z.

Guo, H., M. Xu, and Q. Hu, 2011: Changes in near-surface wind speed in China: 1969–2005. *Int. J. Climatol.*, **31**, 349–358, doi: 10.1002/joc.2091.

Guo, X. Y., L. Wang, L. D. Tian, et al., 2017: Elevation-dependent reductions in wind speed over and around the Tibetan Plateau. *Int. J. Climatol.*, **37**, 1117–1126, doi: 10.1002/joc.4727.

Han, L., J. P. Wang, G. Z. Wang, et al., 2018: Spatial and temporal characteristics of average wind speed in the wind erosion region of northern China. *Arid Land Geogr.*, **41**, 963–971. (in Chinese)

Han, S. J., Q. H. Tang, X. Z. Zhang, et al., 2016: Surface wind observations affected by agricultural development over Northwest China. *Environ. Res. Lett.*, **11**, 054014, doi: 10.1088/1748-9326/11/5/054014.

He, D. Y., H. Tian, and W. T. Deng, 2012: Comparative analysis of the effects of different methods in homogeneity test on annual wind speed. *Trans. Atmos. Sci.*, **35**, 342–349. (in Chinese)

He, Y. P., A. H. Monahan, C. G. Jones, et al., 2010: Probability distributions of land surface wind speeds over North America. *J. Geophys. Res. Atmos.*, **115**, D04103, doi: 10.1029/2008JD010708.

Hou, A. Z., G. C. Ni, H. B. Yang, et al., 2013: Numerical analysis on the contribution of urbanization to wind stilling: An example over the greater Beijing metropolitan area. *J. Appl. Meteor. Climatol.*, **52**, 1105–1115, doi: 10.1175/JAMC-D-12-013.1.

Hu, Y. H., D. Y. Gong, R. Mao, et al., 2019: Relationships between interannual variations of spring winds in the agro-pastoral transitional zone of northern China and winter sea surface temperature. *Prog. Geogr.*, **38**, 709–717, doi: 10.18306/dlkxjz.2019.05.008. (in Chinese)

Huang, H. Y., S. B. Capps, S. C. Huang, et al., 2015: Downscaling near-surface wind over complex terrain using a physically-based statistical modeling approach. *Climate Dyn.*, **44**, 529–542, doi: 10.1007/s00382-014-2137-1.

Jacobson, M. Z., and Y. J. Kaufman, 2006: Wind reduction by aerosol particles. *Geophys. Res. Lett.*, **33**, L24814, doi: 10.1029/2006GL027838.

Jiang, D. B., and Z. P. Tian, 2013: East Asian monsoon change for the 21st century: Results of CMIP3 and CMIP5 models. *Chinese Sci. Bull.*, **58**, 1427–1435, doi: 10.1007/s11434-012-5533-0.

Jiang, Y., Y. Luo, and Z. C. Zhao, 2009: Evaluation of wind speeds in China as simulated by global climate models. *Acta Meteor. Sinica*, **67**, 923–934. (in Chinese)

Jiang, Y., Y. Luo, and Z. C. Zhao, 2010a: Projection of wind speed changes in China in the 21st century by climate models. *Chinese J. Atmos. Sci.*, **34**, 323–336. (in Chinese)

Jiang, Y., Y. Luo, Z. C. Zhao, et al., 2010b: Changes in wind speed over China during 1956–2004. *Theor. Appl. Climatol.*, **99**, 421–430, doi: 10.1007/s00704-009-0152-7.

Jiang, Y., Y. Luo, Z. C. Zhao, et al., 2010c: Projections of wind changes for 21st century in China by three regional climate models. *Chinese Geogr. Sci.*, **20**, 226–235, doi: 10.1007/s11769-010-0226-6.

Jiang, Y., X. Y. Xu, H. W. Liu, et al., 2017: The underestimated magnitude and decline trend in near-surface wind over China. *Atmos. Sci. Lett.*, **18**, 475–483, doi: 10.1002/asl.791.

Jiang, Y., X. Y. Xu, H. W. Liu, et al., 2018: Projection of surface wind by CMIP5 and CMIP3 in China in the 21st century. *J. Meteor. Environ.*, **34**, 56–63. (in Chinese)

Jin, W., G. Y. Ren, Y. Qu, et al., 2012: Change in surface mean wind speed of Northeast China during the period of 1971–2010. *Arid Zone Res.*, **29**, 648–653. (in Chinese)

Kalnay, E., and M. Cai, 2003: Impact of urbanization and land-use change on climate. *Nature*, **423**, 528–531, doi: 10.1038/nature 01675.

Kirchmeier, M. C., D. J. Lorenz, and D. J. Vimont, 2014: Statistical downscaling of daily wind speed variations. *J. Appl. Meteor. Climatol.*, **53**, 660–675, doi: 10.1175/JAMC-D-13-023 0.1.

Li, J., R. C. Yu, and T. J. Zhou, 2008: Seasonal variation of the diurnal cycle of rainfall in southern contiguous China. *J. Climate*, **21**, 6036–6043, doi: 10.1175/2008JCLI2188.1.

Li, J., R. C. Yu, W. H. Yuan, et al., 2011: Changes in duration-related characteristics of late-summer precipitation over eastern China in the past 40 years. *J. Climate*, **24**, 5683–5690, doi: 10.1175/JCLI-D-11-00009.1.

Li, Y., Y. Wang, and J. P. Tang, 2007: Temporal and spatial variety characteristics in near-surface wind energy in China. *J. Nanjing Univ. (Nat. Sci.)*, **43**, 280–291. (in Chinese)

Li, Y., Y. Wang, H. Y. Chu, et al., 2008: The climate influence of anthropogenic land-use changes on near-surface wind energy potential in China. *Chinese Sci. Bull.*, **53**, 2859–2866, doi: 10.1007/s11434-008-0360-z.

Li, Y. J., X. G. He, X. A. Lu, et al., 2018: Spatio–temporal variability of wind speed in the Yangtze River basin during 1960–2015. *Trop. Geogr.*, **38**, 660–667. (in Chinese)

Li, Y. P., Y. N. Chen, Z. Li, et al., 2018: Recent recovery of surface wind speed in northwest China. *Int. J. Climatol.*, **38**, 4445–4458, doi: 10.1002/joc.5679.

Li, Z., Z. W. Yan, K. Tu, et al., 2011: Changes in wind speed and extremes in Beijing during 1960–2008 based on homogenized observations. *Adv. Atmos. Sci.*, **28**, 408–420, doi: 10.1007/s00376-010-0018-z.

Li, Z. C., Z. G. Wei, and R. Gao, 2004: Spatial and temporal characters of surface wind in Gansu Corridor Oasis in recent 50 years. *Plateau Meteor.*, **23**, 259–263. (in Chinese)

Li, Z. Q., W. K. M. Lau, V. Ramanathan, et al., 2016: Aerosol and monsoon climate interactions over Asia. *Rev. Geophys.*, **54**, 866–929, doi: 10.1002/2015RG000500.

Li, Z. Q., L. L. Song, H. Ma, et al., 2018: Observed surface wind speed declining induced by urbanization in East China. *Climate Dyn.*, **50**, 735–749, doi: 10.1007/s00382-017-3637-6.

Lim, Y. K., M. Cai, E. Kalnay, et al., 2005: Observational evidence of sensitivity of surface climate changes to land types and urbanization. *Geophys. Res. Lett.*, **32**, L22712, doi: 10.1029/2005GL024267.

Lin, C. G., K. Yang, J. Qin, et al., 2013: Observed coherent trends of surface and upper-air wind speed over China since 1960. *J. Climate*, **26**, 2891–2903, doi: 10.1175/JCLI-D-12-00093.1.

Lin, C. G., K. Yang, J. P. Huang, et al., 2015: Impacts of wind stilling on solar radiation variability in China. *Sci. Rep.*, **5**, 15135, doi: 10.1038/srep15135.

Liu, H. Z., C. C. Xu, J. X. Li, et al., 2017: Changes in the maximum wind speed and the confirmatory analysis by the circulation index in Xinjiang Region. *Yellow River*, **39**, 19–25. (in Chinese)

Liu, M., Y. J. Shen, Y. Zeng, et al., 2010: Trend in pan evaporation and its attribution over the past 50 years in China. *J. Geogr. Sci.*, **20**, 557–568, doi: 10.1007/s11442-010-0557-3.

Liu, M. L., and H. Q. Tian, 2010: China's land cover and land use change from 1700 to 2005: Estimations from high-resolution satellite data and historical archives. *Global Biogeochem. Cycles*, **24**, GB3003, doi: 10.1029/2009GB003687.

Liu, X., X. J. Zhang, Q. Tang, et al., 2014: Effects of surface wind speed decline on modeled hydrological conditions in China. *Hydrol. Earth Syst. Sci.*, **18**, 2803–2813, doi: 10.5194/hess-18-2803-2014.

Liu, X. N., 2000: The homogeneity test on mean annual wind speed over China. *Quart. J. Appl. Meteor.*, **11**, 27–34. (in Chinese)

Liu, X. M., Y. Z. Luo, D. Zhang, et al., 2011a: Recent changes in pan-evaporation dynamics in China. *Geophys. Res. Lett.*, **38**, L13404, doi: 10.1029/2011GL047929.

Liu, X. M., H. X. Zheng, M. H. Zhang, et al., 2011b: Identification of dominant climate factor for pan evaporation trend in the Tibetan Plateau. *J. Geogr. Sci.*, **21**, 594–608, doi: 10.1007/s11442-011-0866-1.

Mahowald, N. M., S. Engelstaedter, C. Luo, et al., 2009: Atmospheric iron deposition: Global distribution, variability, and human perturbations. *Ann. Rev. Mar. Sci.*, **1**, 245–278, doi: 10.1146/annurev.marine.010908.163727.

McInnes, K. L., T. A. Erwin, and J. M. Bathols, 2011: Global Climate Model projected changes in 10 m wind speed and direction due to anthropogenic climate change. *Atmos. Sci. Lett.*, **12**, 325–333, doi: 10.1002/asl.341.

McMahon, T. A., M. C. Peel, L. Lowe, et al., 2013: Estimating actual, potential, reference crop and pan evaporation using standard meteorological data: a pragmatic synthesis. *Hydrol. Earth Syst. Sci.*, **17**, 1331–1363, doi: 10.5194/hess-17-1331-2013.

McVicar, T. R., and M. L. Roderick, 2010: Atmospheric science: Winds of change. *Nat. Geosci.*, **3**, 747–748, doi: 10.1038/ngeo1002.

McVicar, T. R., T. G. Van Niel, L. T. Li, et al., 2008: Wind speed climatology and trends for Australia, 1975–2006: Capturing the stilling phenomenon and comparison with near-surface reanalysis output. *Geophys. Res. Lett.*, **35**, L20403, doi: 10.1029/2008GL035627.

McVicar, T. R., T. G. Van Niel, M. L. Roderick, et al., 2010: Observational evidence from two mountainous regions that near-surface wind speeds are declining more rapidly at higher elevations than lower elevations: 1960–2006. *Geophys. Res. Lett.*, **37**, L06402, doi: 10.1029/2009GL042255.

McVicar, T. R., M. L. Roderick, R. J. Donohue, et al., 2012a: Global review and synthesis of trends in observed terrestrial near-surface wind speeds: Implications for evaporation. *J. Hydrol.*, **416–417**, 182–205, doi: 10.1016/j.jhydrol.2011.10.024.

McVicar, T. R., M. L. Roderick, R. J. Donohue, et al., 2012b: Less bluster ahead? Ecohydrological implications of global trends of terrestrial near-surface wind speeds *Ecohydrology*, **5**, 381–388, doi: 10.1002/eco.1298.

Najac, J., C. Lac, and L. Terray, 2011: Impact of climate change on surface winds in France using a statistical–dynamical downscaling method with mesoscale modelling. *Int. J. Climatol.*, **31**, 415–430, doi: 10.1002/joc.2075.

Niyogi, D., P. Pyle, M. Lei, et al., 2011: Urban modification of thunderstorms: An observational storm climatology and model case study for the Indianapolis urban region. *J. Appl. Meteor. Climatol.*, **50**, 1129–1144, doi: 10.1175/2010JAMC1836.1.

Peterson, T. C., D. R. Easterling, T. R. Karl, et al., 1998: Homo-

geneity adjustments of in situ atmospheric climate data: A review. *Int. J. Climatol.*, **18**, 1493–1517, doi: 10.1002/(SICI)1097-0088(19981115)18:13<1493::AID-JOC329>3.0.CO;2-T.

Pryor, S. C., and R. J. Barthelmie, 2011: Assessing climate change impacts on the near-term stability of the wind energy resource over the United States. *Proc. Natl. Acad. Sci. USA*, **108**, 8167–8171, doi: 10.1073/pnas.1019388108.

Pryor, S. C., R. J. Barthelmie, D. T. Young, et al., 2009: Wind speed trends over the contiguous United States. *J. Geophys. Res. Atmos.*, **114**, D14105, doi: 10.1029/2008JD011416.

Pryor, S. C., R. J. Barthelmie, M. S. Bukovsky, et al., 2020: Climate change impacts on wind power generation. *Nat. Rev. Earth Environ.*, **1**, 627–643, doi: 10.1038/s43017-020-0101-7.

Qian, C., and W. X. Zhang, 2019: Short commentary on CMIP6 Detection and Attribution Model Intercomparison Project (DAMIP). *Climate Change Res.*, **15**, 469–475. (in Chinese)

Rayner, D. P., 2007: Wind run changes: The dominant factor affecting pan evaporation trends in Australia. *J. Climate*, **20**, 3379–3394, doi: 10.1175/JCLI4181.1.

Ren, G. Y., J. Guo, M. Z. Xu, et al., 2005: Climate changes of China's mainland over the past half century. *Acta Meteor. Sinica*, **63**, 942–956. (in Chinese)

Roderick, M. L., L. D. Rotstayn, G. D. Farquhar, et al., 2007: On the attribution of changing pan evaporation. *Geophys. Res. Lett.*, **34**, L17403, doi: 10.1029/2007GL031166.

Sherman, P., X. Y. Chen, and M. B. McElroy, 2017: Wind-generated electricity in China: Decreasing potential, inter-annual variability and association with changing climate. *Sci. Rep.*, **7**, 16294, doi: 10.1038/s41598-017-16073-2.

Shi, P. J., G. F. Zhang, K. Feng, et al., 2015: Wind speed change regionalization in China (1961–2012). *Adv. Climate Change Res.*, **6**, 151–158, doi: 10.1016/j.accre.2015.09.006.

Sterk, H. A. M., G. J. Steeneveld, T. Vihma, et al., 2015: Clear-sky stable boundary layers with low winds over snow-covered surface. Part 1: WRF model evaluation. *Quart. J. Roy. Meteor. Soc.*, **141**, 2165–2184, doi: 10.1002/qj.2513.

Tang, B., L. Tong, S. Z. Kang, et al., 2011: Impacts of climate variability on reference evapotranspiration over 58 years in the Haihe river basin of north China. *Agric. Water Manag.*, **98**, 1660–1670, doi: 10.1016/j.agwat.2011.06.006.

Troccoli, A., K. Muller, P. Coppin, et al., 2012: Long-term wind speed trends over Australia. *J. Climate*, **25**, 170–183, doi: 10.1175/2011JCLI4198.1.

Vautard, R., J. Cattiaux, P. Yiou, et al., 2010: Northern Hemisphere atmospheric stilling partly attributed to an increase in surface roughness. *Nat. Geosci.*, **3**, 756–761, doi: 10.1038/ngeo979.

Wan, H., X. L. Wang, and V. R. Swail, 2010: Homogenization and trend analysis of Canadian near-surface wind speeds. *J. Climate*, **23**, 1209–1225, doi: 10.1175/2009JCLI3200.1.

Wang, J., J. M. Feng, Z. W. Yan, et al., 2020: An analysis of the urbanization contribution to observed terrestrial stilling in the Beijing–Tianjin–Hebei region of China. *Environ. Res. Lett.*, **15**, 032062, doi: 10.1088/1748-9326/ab7396.

Wang, X. M., J. B. Liao, J. Zhang, et al., 2013: A numeric study of regional climate change induced by urban expansion in the Pearl River Delta, China. *J. Appl. Meteor. Climatol.*, **53**, 346–362, doi: 10.1175/JAMC-D-13-054.1.

Wang, Z. Y., Y. H. Ding, J. H. He, et al., 2004: An updating analysis of the climate change in China in recent 50 years. *Acta Meteor. Sinica*, **62**, 228–236. (in Chinese)

Wu, J., J. Guo, and D. M. Zhao, 2013: Characteristics of aerosol transport and distribution in East Asia. *Atmos. Res.*, **132–133**, 185–198, doi: 10.1016/j.atmosres.2013.05.018.

Wu, J., J. L. Zha, and D. M. Zhao, 2016: Estimating the impact of the changes in land use and cover on the surface wind speed over the East China Plain during the period 1980–2011. *Climate Dyn.*, **46**, 847–863, doi: 10.1007/s00382-015-2616-z.

Wu, J., J. L. Zha, and D. M. Zhao, 2017: Evaluating the effects of land use and cover change on the decrease of surface wind speed over China in recent 30 years using a statistical downscaling method. *Climate Dyn.*, **48**, 131–149, doi: 10.1007/s00382-016-3065-z.

Wu, J., J. L. Zha, D. M. Zhao, et al., 2018a: Changes in terrestrial near-surface wind speed and their possible causes: an overview. *Climate Dyn.*, **51**, 2039–2078, doi: 10.1007/s00382-017-3997-y.

Wu, J., J. L. Zha, D. M. Zhao, et al., 2018b: Changes of wind speed at different heights over eastern China during 1980–2011. *Int. J. Climatol.*, **38**, 4476–4495, doi: 10.1002/joc.5681.

Wu, J., J. L. Zha, D. M. Zhao, et al., 2018c: Effects of surface friction and turbulent mixing on long-term changes in the near-surface wind speed over the Eastern China Plain from 1981 to 2010. *Climate Dyn.*, **51**, 2285–2299, doi: 10.1007/s00382-017-4012-3.

Xu, M., C. P. Chang, C. B. Fu, et al., 2006: Steady decline of east Asian monsoon winds, 1969–2000: Evidence from direct ground measurements of wind speed. *J. Geophys. Res. Atmos.*, **111**, D24111, doi: 10.1029/2006JD007337.

Xu, Y. Y., S. H. Liu, F. Hu, et al., 2009: Influence of Beijing urbanization on the characteristics of atmospheric boundary layer. *Chinese J. Atmos. Sci.*, **33**, 859–867. (in Chinese)

Yang, J. B., Q. Y. Liu, X. Li, et al., 2017: Overview of wind power in China: Status and future. *Sustainability*, **9**, 1454, doi: 10.3390/su9081454.

Yang, K., B. S. Ye, D. G. Zhou, et al., 2011: Response of hydrological cycle to recent climate changes in the Tibetan Plateau. *Climatic Change*, **109**, 517–534, doi: 10.1007/s10584-011-0099-4.

Yang, X. M., Z. X. Li, Q. Feng, et al., 2012: The decreasing wind speed in southwestern China during 1969–2009, and possible causes. *Quat. Int.*, **263**, 71–84, doi: 10.1016/j.quaint.2012.02.020.

Yin, Y. H., S. H. Wu, G. Chen, et al., 2010a: Attribution analyses of potential evapotranspiration changes in China since the 1960s. *Theor. Appl. Climatol.*, **101**, 19–28, doi: 10.1007/s00704-009-0197-7.

Yin, Y. H., S. H. Wu, and E. F. Dai, 2010b: Determining factors in potential evapotranspiration changes over China in the period 1971–2008. *Chinese Sci. Bull.*, **55**, 3329–3337, doi: 10.1007/s11434-010-3289-y.

You, Q. L., S. C. Kang, W. A. Flügel, et al., 2010: Decreasing wind speed and weakening latitudinal surface pressure gradients in the Tibetan Plateau. *Climate Res.*, **42**, 57–64, doi: 10.3354/cr00864.

Yu, R. C., J. Li, and H. M. Chen, 2009: Diurnal variation of surface wind over central eastern China. *Climate Dyn.*, **33**, 1089, doi: 10.1007/s00382-008-0478-3.

Yu, R. C., W. H. Yuan, J. Li, et al., 2010: Diurnal phase of late-

night against late-afternoon of stratiform and convective precipitation in summer southern contiguous China. *Climate Dyn.*, **35**, 567–576, doi: 10.1007/s00382-009-0568-x.

Yu, R. C., J. Li, H. M. Chen, et al., 2014: Progress in studies of the precipitation diurnal variation over contiguous China. *J. Meteor. Res.*, **28**, 877–902, doi: 10.1007/s13351-014-3272-7.

Zeng, Z. Z., A. D. Ziegler, T. Searchinger, et al., 2019: A reversal in global terrestrial stilling and its implications for wind energy production. *Nat. Climate Change*, **9**, 979–985, doi: 10.1038/s41558-019-0622-6.

Zha, J. L., J. Wu, and D. M. Zhao, 2016: Changes of probabilities in different wind grades induced by land use and cover change in Eastern China Plain during 1980–2011. *Atmos. Sci. Lett.*, **17**, 264–269, doi: 10.1002/asl.653.

Zha, J. L., J. Wu, and D. M. Zhao, 2017a: Effects of land use and cover change on the near-surface wind speed over China in the last 30 years. *Prog. Phys. Geog.*, **41**, 46–67, doi: 10.1177/0309133316663097.

Zha, J. L., J. Wu, D. M. Zhao, et al., 2017b: Changes of the probabilities in different ranges of near-surface wind speed in China during the period for 1970–2011. *J. Wind Eng. Ind. Aerod.*, **169**, 156–167, doi: 10.1016/j.jweia.2017.07.019.

Zha, J. L., J. Wu, D. M. Zhao, et al., 2019a: A possible recovery of the near-surface wind speed in Eastern China during winter after 2000 and the potential causes. *Theor. Appl. Climatol.*, **136**, 119–134, doi: 10.1007/s00704-018-2471-z.

Zha, J. L., D. M. Zhao, J. Wu, et al., 2019b: Numerical simulation of the effects of land use and cover change on the near-surface wind speed over Eastern China. *Climate Dyn.*, **53**, 1783–1803, doi: 10.1007/s00382-019-04737-w.

Zha, J. L., J. Wu, D. M. Zhao, et al., 2020: Future projections of the near-surface wind speed over eastern China based on CMIP5 datasets. *Climate Dyn.*, **54**, 2361–2385, doi: 10.1007/s00382-020-05118-4.

Zhang, A. Y., G. Y. Ren, J. Guo, et al., 2009: Change trend analyses on upper-air wind speed over China in past 30 years. *Plateau Meteor.*, **28**, 680–687. (in Chinese)

Zhang, D. H., J. Q. Wang, Y. G. Lin, et al., 2017: Present situation and future prospect of renewable energy in China. *Renew. Sustain. Energy Rev.*, **76**, 865–871, doi: 10.1016/j.rser.2017.03.023.

Zhang, G. F., C. Azorin-Molina, P. J. Shi, et al., 2019: Impact of near-surface wind speed variability on wind erosion in the eastern agro-pastoral transitional zone of Northern China, 1982–2016. *Agric. Forest. Meteorol.*, **271**, 102–115, doi: 10.1016/j.agrformet.2019.02.039.

Zhang, G. F., C. Azorin-Molina, D. L. Chen, et al., 2020: Variability of daily maximum wind speed across China, 1975–2016: An examination of likely causes. *J. Climate*, **33**, 2793–2816, doi: 10.1175/JCLI-D-19-0603.1.

Zhang, J. Q., C. L. Zhang, C. P. Chang, et al., 2017: Comparison of wind erosion based on measurements and SWEEP simulation: A case study in Kangbao County, Hebei Province, China. *Soil Tillage Res.*, **165**, 169–180, doi: 10.1016/j.still.2016.08.006.

Zhang, N., Z. Q. Gao, X. M. Wang, et al., 2010: Modeling the impact of urbanization on the local and regional climate in Yangtze River Delta, China. *Theor. Appl. Climatol.*, **102**, 331–342, doi: 10.1007/s00704-010-0263-1.

Zhang, N., X. M. Wang, Y. Chen, et al., 2015: Numerical simulations on influence of urban land cover expansion and anthropogenic heat release on urban meteorological environment in Pearl River Delta. *Theor. Appl. Climatol.*, **126**, 469–479, doi: 10.1007/s00704-015-1601-0.

Zhang, R. H., S. Y. Zhang, J. L. Luo, et al., 2019: Analysis of near-surface wind speed change in China during 1958–2015. *Theor. Appl. Climatol.*, **137**, 2785–2801, doi: 10.1007/s00704-019-02769-0.

Zhang, Y., L. N. Gao, L. J. Cao, et al., 2020: Decreasing atmospheric visibility associated with weakening winds from 1980 to 2017 over China. *Atmos. Environ.*, **224**, 117314, doi: 10.1016/j.atmosenv.2020.117314.

Zhang, Y. Q., C. M. Liu, Y. H. Tang, et al., 2007: Trends in pan evaporation and reference and actual evapotranspiration across the Tibetan Plateau. *J. Geophys. Res. Atmos.*, **112**, D12110, doi: 10.1029/2006JD008161.

Zhang, Z. T., and K. C. Wang, 2020: Stilling and recovery of the surface wind speed based on observation, reanalysis, and geostrophic wind theory over China from 1960 to 2017. *J. Climate*, **33**, 3989–4008, doi: 10.1175/JCLI-D-19-0281.1.

Zhang, Z. T., K. C. Wang, D. L. Chen, et al., 2019: Increase in surface friction dominates the observed surface wind speed decline during 1973–2014 in the Northern Hemisphere lands. *J. Climate*, **32**, 7421–7435, doi: 10.1175/JCLI-D-18-0691.1.

Zhao, D. M., and J. Wu, 2017a: The influence of urban surface expansion in China on regional climate. *J. Climate*, **30**, 1061–1080, doi: 10.1175/JCLI-D-15-0604.1.

Zhao, D. M., and J. Wu, 2017b: Inclusion of land use changes in long-term regional climate simulations over East Asia. *Atmos. Sci. Lett.*, **18**, 187–192, doi: 10.1002/asl.744.

Zhao, M., and X. M. Zeng, 2002: A theoretical analysis on the local climate change induced by the change of landuse. *Adv. Atmos. Sci.*, **19**, 45–63, doi: 10.1007/s00376-002-0033-9.

Zhao, Z. C., Y. Luo, Y. Jiang, et al., 2016: Possible reasons of wind speed decline in China for the last 50 years. *Adv. Meteor. Sci. Technol.*, **6**, 106–109. (in Chinese)

Zheng, H. X., X. M. Liu, C. M. Liu, et al., 2009: Assessing contributions to panevaporation trends in Haihe River Basin, China. *J. Geophys. Res. Atmos.*, **114**, D24105, doi: 10.1029/2009JD012203.

Zheng, J. Y., J. J. Bian, Q. S. Ge, et al., 2013: The climate regionalization in China for 1981–2010. *Chinese Sci. Bull.*, **58**, 3088–3099, doi: 10.1360/972012-1491.

Zhou, B. Y., F. Zheng, and J. Zhu, 2017: Analysis of the interannual variations and influencing factors of wind speed anomalies over the Beijing–Tianjin–Hebei region. *Atmos. Ocean. Sci. Lett.*, **10**, 312–318, doi: 10.1080/16742834.2017.1327301.

Tech & Copy Editor: Meili ZHANG